1/f NOISE AND RELATED SURFACE EFFECTS IN GERMANIUM

by

ALAN LOUIS McWHORTER

B.S., University of Illinois
(1951)

SUBMITTED IN PARTIAL FULFILLMENT OF THE

REQUIREMENTS FOR THE DEGREE OF

DOCTOR OF SCIENCE

at the

MASSACHUSETTS INSTITUTE OF TECHNOLOGY

June, 1955

Signature of Author -
Department of Electrical Engineering, May 16, 1955

Certified by -
Thesis Supervisor

Accepted by -
Chairman, Departmental Committee on Graduate Students

EE
Thesis
1955

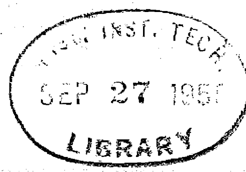

1/f NOISE AND RELATED SURFACE EFFECTS IN GERMANIUM

by

ALAN LOUIS McWHORTER

Submitted to the Department of Electrical Engineering on May 16, 1955, in partial fulfillment of the requirements for the degree of Doctor of Science.

ABSTRACT

Recent experiments on germanium surfaces have shown that in addition to the surface recombination centers there exists a class of surface states, or traps, which possess a relaxation time of the order of seconds or minutes and a density greater than $10^{13}/cm^2$. By modulating the surface conductivity with external electric fields ("field effect" experiment) at sub-audio frequencies, it has been found that the capture time τ of these traps varies from spot to spot along the surface, with a distribution function for τ which is approximately proportional to $1/\tau$ up to times greater than 100 sec. It is proposed that 1/f noise in germanium filaments arises from a fluctuation in the occupancy of these traps. The filling and emptying of the traps can alter the conductivity by producing (1) changes in the majority carrier concentration near the surface, as required to maintain charge neutrality, and (2) an injection-extraction of hole-electron pairs, due to a complex interaction between the surface recombination centers and the traps. Using only the information supplied by the field effect experiment, the two processes have been analyzed and found to give a 1/f noise of the correct order of magnitude. To obtain this quantitative result, it is sufficient to specify only the dimensions of the sample and the bulk and surface potentials; neither the origin of the $1/\tau$ distribution nor the trap energy level and density need be known. Because of the long capture times, it is necessary to assume that the traps are located in or on the oxide layer, separated from the germanium by a potential barrier. The observed temperature insensitivity of the time constants suggests that electrons communicate with the traps by tunneling through the barrier, in which case a $1/\tau$ distribution would result from an approximately uniform distribution of barrier heights or widths. The latter may occur in a natural manner either from a homogeneous distribution of the traps throughout the oxide layer, or, if the traps are produced by adsorbed ions, from a small variation of the oxide thickness over the surface.

There are two distinct types of excess reverse currents observed in p-n junctions: a water-induced leakage current, which flows externally to the germanium, and a "channel" current, which occurs whenever a strongly n- or p-type surface increases the effective rectifying area of the junction. Measurements of 1/f noise in reverse-biased p-n junctions have shown that the noise associated with the leakage current varies roughly at V^2G, where V is the applied voltage and G is the conductance of the leakage path, while the noise associated with the channel seems to vary as $I_c{}^2V^{1/2}$, where I_c is the channel current. The first relation suggests that the leakage path is composed of many parallel paths, each of whose conductance fluctuates independently. The channel noise may be caused by fluctuations in the rate of generation of hole-electron pairs at the surface or by fluctuations in the surface conductivity. By combining the proposed 1/f noise theory with a somewhat imperfect model of the channel, it has been possible to analyze

both mechanisms. While neither calculation leads to exactly the empirical $I_c^2V^{1/2}$ relation, the one based on conductivity fluctuations gives a larger value for the noise which is of the right order of magnitude.

Although most of the devices exhibiting 1/f noise differ from germanium filaments in that the current passes through potential barriers, essentially the same model may still apply. Fluctuations in the resistance can be produced by traps located in the barrier region, since a variation in the trapped charge will cause a variation in the height of the barrier. If the trap communicates with the bulk by electrons tunneling through the barrier, then a 1/f spectrum will be obtained if the traps are simply distributed uniformly throughout the barrier region. This idea has been explored by using the thin oxide layer on aluminum to form a potential barrier between the base metal and a mercury drop. It has been found that such contacts produce a large 1/f noise with the usual characteristics and that a tunneling process is suggested by the temperature independence of the dc resistance, but the experiments have not been carried far enough to establish the noise model.

Thesis Supervisor: Richard B. Adler
Title: Associate Professor of Electrical Engineering

ACKNOWLEDGMENT

The author wishes to thank Professor R. B. Adler and Professor J. E. Thomas, Jr. for their helpful advice and criticism throughout the present work. He is especially indebted to R. H. Kingston both for many stimulating discussions as well as for actual collaboration on much of the experimental work. M. Green is also to be thanked for several suggestions regarding experimental technique and for a number of discussions of the physical chemistry of germanium surfaces.

TABLE OF CONTENTS

Abstract		iii
Acknowledgement		v
Chapter I.	INTRODUCTION	1
Chapter II.	RELAXATION TIME OF SURFACE STATES IN GERMANIUM	17
Chapter III.	1/f NOISE IN GERMANIUM FILAMENTS	32
Chapter IV.	CHANNELS AND EXCESS REVERSE CURRENT IN p-n JUNCTIONS	51
Chapter V.	1/f NOISE IN p-n JUNCTIONS	69
Chapter VI.	EXTENSION OF NOISE MODEL	88
Appendix A		96
Appendix B		100
Appendix C		105
References		110

CHAPTER I

INTRODUCTION

As is well known, all resistive devices in thermal equilibrium show a mean-square voltage fluctuation across their terminals equal to $4kTR\Delta f$ in any frequency interval Δf (at least up to the infrared regions). In general, the application of a dc voltage or current will result in an additional amount of noise. Two classes of non-equilibrium fluctuations which are frequently observed under such circumstances and which have been the subject of much experimental and theoretical study are shot noise and $1/f$ noise.

Although we will not be concerned with shot noise here, it may be well to mention that the term is now applied to a much wider class of fluctuations than just the random emission of electrons from the cathode of a vacuum tube. The analogous current fluctuation in a point-contact or p-n junction rectifier is called shot noise, and the name is also commonly used to describe the noise produced by random fluctuations in the number of charge carriers in a semiconductor.[1] The power spectrum associated with shot noise is flat out to the reciprocal of some characteristic time (e.g., the transit time of the electrons in a vacuum tube or the lifetime of the carriers in a semiconductor) and then falls off with increasing frequency.

In contrast to this type of spectrum, many devices when biased with a dc current show an excess noise power which roughly obeys a $1/f^n$ law, where n is approximately unity (1 to 1.5). Such a spectrum was first observed in vacuum tubes, where it is known as "flicker noise"; but it also occurs, for example, in carbon microphones and resistors, thin metallic films, point-contact diodes and transistors, junction diodes and transistors, and even single-crystal germanium filaments. In carbon microphones and resistors

this noise is called "contact noise", because it appears to arise at the contacts between the carbon grains, but the whole class of such fluctuations is generally known as "1/f noise" or "excess noise". Two other significant characteristics of this type of noise are that the mean-square voltage fluctuation increases approximately with the square of the dc biasing current and that the amplitude is not strongly temperature dependent. Because of the current dependence, 1/f noise is usually interpreted as a resistance fluctuation.

The frequency range over which the approximate 1/f law holds is truly remarkable. Although it cannot be obeyed over an infinite range because the total power must be finite, no low-frequency or high-frequency cutoff points have ever been observed for any of the above devices. Rollin and Templeton[2] have measured the noise for both carbon resistors and germanium filaments down to 2.5×10^{-4} cps and found no significant deviation from a $1/f^n$ spectrum. For point-contact diodes measurements have recently been pushed down to 6×10^{-5} cps with the same observation.[3] At the other end of the spectrum, the 1/f noise appears to fall below thermal or shot noise before the high-frequency cutoff point occurs. For carbon resistors[4] and point-contact rectifiers,[5] however, the 1/f noise is often still dominant at 1 Mc. In these two cases one must therefore account for a 1/f law over at least 10 or 11 decades of frequency.

Equally as remarkable is the temperature range over which 1/f noise is observed. Templeton and MacDonald[6] measured the noise in carbon resistors from 290°K to 4.2°K over a frequency range from 20 cps to 10 kc. Not only did they find that the 1/f noise still existed at these low temperatures, but also that the magnitude did not vary by more than a factor of ten over

the entire temperature range. Russel[7] had previously reported that noise measurements between 100 and 5×10^5 cps on ZnO crystals at liquid helium temperature showed a 1/f spectrum with an amplitude insensitive to temperature. Several other sources of 1/f noise, including point-contact rectifiers[8] and germanium filaments,[9] have been measured down to liquid nitrogen temperature (77°K) with similar results. In the case of germanium filaments, Gebbie[10] has recently found at low temperatures a shot noise spectrum, apparently due to a trapping process, superimposed on the 1/f spectrum. Although this means that one must be very careful in interpreting low-temperature measurements on semiconductors, Gebbie's results are still in agreement with the general observation that 1/f noise noise is not strongly temperature dependent.

The similarity of the 1/f noise from the various devices mentioned above of course leads one to look for a common mechanism; but so far there has not been a really satisfactory explanation for even one of them. The basic difficulty is that a 1/f spectrum, in contrast to a shot noise spectrum, does not appear to be characteristic of any elementary process. In fact many of the physically reasonable mechanisms for modulating the resistance give just a shot noise spectrum. However, it has been known for some time that by superimposing shot noise spectra of the type $\tau/\left[1 + (\omega\tau)^2\right]$, with a distribution function for the time constant τ which is proportional to $1/\tau$, a 1/f spectrum can be obtained.[11] Since the 1/f law may be obeyed over 10 decades or more of frequency, this approach requires that the $1/\tau$ distribution of time constants cover a correspondingly large range. One plausible way to achieve the desired result, which was proposed at about the same time by van der Ziel[12] and duPré[13], will be outlined next.

Suppose that the time constants arise from a process involving an activation energy, such as the adsorption-desorption of an ion or the diffusion of an ion, so that τ is of the form

$$\tau = \tau_o \exp(E/kT), \tag{1.1}$$

where E is the activation energy. A uniform distribution of energies between E_1 and E_2 will then correspond to a $1/\tau$ distribution for τ between $\tau_1 = \exp(E_1/kT)$ and $\tau_2 = \exp(E_2/kT)$. Hence if the noise is produced by a large number of independent processes, each of which gives a shot noise spectrum of the form $\tau/\left[1 + (\omega\tau)^2\right]$, with τ distributed as just described, then the total power spectrum will be

$$G(\omega) \propto \int_{\tau_1}^{\tau_2} \frac{1}{\tau} \frac{\tau}{1 + (\omega\tau)^2} d\tau \Big/ \int_{\tau_1}^{\tau_2} \frac{1}{\tau} d\tau$$

$$= \frac{kT}{E_2 - E_1} \frac{1}{\omega} (\tan^{-1} \omega\tau_2 - \tan^{-1} \omega\tau_1) . \tag{1.2}$$

If in the frequency range under consideration $\omega\tau_1 \ll 1 \ll \omega\tau_2$, then

$$G(\omega) \propto \frac{kT}{E_2 - E_1} \frac{1}{\omega} . \tag{1.3}$$

Although both τ_1 and τ_2 are exponentially dependent on the temperature, the power spectrum will only be linearly dependent on T if

$$E_1 \ll kT \ln(1/\omega\tau_o)$$
$$E_2 \gg kT \ln(1/\omega\tau_o) \tag{1.4}$$

in the frequency and temperature range under consideration.

As simple as these two requirements may appear, the first one cannot be met at very low temperatures by ionic processes. For the parameter τ_o in this case cannot be smaller than the reciprocal of the "jumping frequency",

which is of the order of 10^{13}/sec.[14] The value of τ in (1.1) would then correspond to the time that it takes a diffusing ion to make a single jump or the time that an adsorbed ion remains on the surface. From (1.4) we find that just to explain the room temperature measurements up to a frequency of 1 Mc, we need $E_1 < 0.35$ ev. But the 1/f spectrum has been measured up to that same frequency at liquid nitrogen temperature and past 10 kc at liquid helium temperature. To account for the liquid nitrogen data we would have to have $E_1 < 0.09$ ev and for the liquid helium data $E_1 < 0.007$ ev. Since the last figure is more than an order of magnitude smaller than activation energies for highly mobile ions diffusing on the surface, and two orders of magnitude smaller than values for bulk diffusion, we can immediately rule out such processes. The same conclusion holds for adsorption-desorption processes, although in this case there is no need to go through any calculation—all of the other gases liquify before helium.

Thus far the discussion has been for 1/f noise which was built up from a superposition of shot noise spectra. By using what appear to be highly specialized models, Richardson[15] and Bess[16] have been able to get 1/f spectra directly from ionic diffusion processes. However, regardless of the detailed workings of a particular model, it is apparent on physical grounds that if E_1 is the minimum activation energy involved in the diffusion process and ν is the jumping frequency, then the most rapid fluctuations cannot have a time constant smaller than the order of $(1/\nu)\exp(E_1/kT)$. Hence the 1/f spectrum must begin to cut off at frequencies of the order of $\omega = \nu \exp(-E_1/kT)$, which leads to exactly the same results as before. Perhaps in some devices at higher temperatures an ionic process may play an important role. But if one is looking for a

single model to explain all 1/f noise, then diffusion or adsorption of ions can be eliminated.

It should be mentioned that Macfarlane[17] had at one time proposed a diffusion mechanism which, with a single activation energy E, apparently gave a 1/f-like spectrum extending indefinitely far above $\omega = \nu \exp(-E/kT)$. This paper contained an error which was pointed out by Burgess;[18] the corrected spectrum does not resemble a 1/f law over any frequency range.

1/f Noise in Germanium

One wholly electronic mechanism for 1/f noise was proposed by Shockley[19] to explain Montgomery's data for germanium filaments.[9] Montgomery had found strong evidence that the resistance modulation was due to a fluctuating minority carrier concentration. The noise amplitude was affected by magnetic fields in a way which corresponded to the change in the lifetime of the minority carriers, and the noise voltages measured across two adjacent segments of the filament were correlated with a time lag of approximately the minority carrier transit time.

For discussion purposes let us consider the case of an n-type filament. Shockley proposed that the fluctuation in the hole concentration might arise from the injection of hole-electron pairs from regions which were less n-type than the neighboring parts of the crystal, or which were actually p-type inclusions. Such injection will take place if these regions contain recombination centers, for an applied field will sweep out the excess holes and thus reduce the recombination rate. Since the generation rate remains constant, the region acts as a natural source of hole-electron pairs. So far this would only give a shot noise spectrum. However, Shockley pointed out that the ability of a recombination center to absorb or emit hole-electron

pairs can be modulated by the emptying and filling of an adjacent trap. If one could obtain a 1/f spectrum for the trap modulation, then the regions would produce a 1/f noise.[20] It was implied that a uniform distribution of energy levels for the traps gave the desired result. But as is shown in Appendix A, this procedure will not lead to a 1/f spectrum if the traps act independently and if one is trying to get the distribution in time constants from the variation in activation energy for the release of a trapped carrier. The reason is that the trapping and releasing of a carrier is a two-parameter process, which does not give rise to just a $\tau / \left[1 + (\omega\tau)^2\right]$ spectrum.

Since the model which will be proposed later borrows some of Shockley's ideas, we will discuss his theory in more detail at that time. One additional point should be mentioned now, however. Montgomery made his original measurements before Herzog and van der Ziel[21] had reported experimental evidence for shot noise in germanium filaments. The effects of shot and 1/f noise are therefore not separated in Montgomery's published results. When the experiments were repeated, exercising proper precautions to insure that only 1/f noise was being measured, he was unable to get consistent results from the magnetic-field experiments. The correlation effect apparently still existed, but the delay time could not be compared with the transit time of the minority carriers under the revised experimental conditions.[22]

It seems quite clear at the present time that 1/f noise in germanium single crystals is predominantly a surface phenomenon; in fact there is every reason to believe that it is entirely so. The now-questionable magnetic-field experiments, and other work of Montgomery, had suggested that the surface was the origin of the noise, but more recent results leave little

doubt. For example, Maple, Bess and Gebbie[23] have found that a 10 to 20 db increase in 1/f noise, with no accompanying increase in the filament lifetime, may be produced by switching a filament from a dry nitrogen ambient to one of carbon tetrachloride. They have also obtained changes of several db in going from dry to wet ambients. In other cases, apparent changes in the shape of the spectrum were observed. The effect of surface treatment on noise magnitude is even more striking in point-contact rectifiers or p-n junctions. Kennedy[24] was able simultaneously to ruin the rectification characteristics and greatly increase the noise in reverse-biased junctions by such techniques as heating the diode or changing the ambient gas. However, the unit could always be restored to its former condition merely by re-etching, indicating that only surface changes had occurred. Furthermore, he found that if he placed a freshly etched and washed junction in a vacuum while it was still wet, the junction was far less noisy than if it had been allowed to dry in the open air first. In Chapter V we will present some measurements for p-n junctions which show that only a small change in the relative humidity can increase the noise level by 30 db or more.

Even without this experimental evidence, one might have looked to the surface for an expalanation of the 1/f noise, simply because it does not seem possible to obtain the required range of correlation times from the bulk. For ionic diffusion processes we have already shown that activation energies as low as 0.1 ev would be necessary to account for the high-frequency data at liquid nitrogen temperature. This is far too small for bulk diffusion in single crystals. The only electronic process which has been found to give the very long times needed for 1/f noise is trapping. In luminescence and photoconductivity work, trapping times of hours and days

have been observed from some semiconductors. However, for germanium no such times as these have ever been reported for bulk trapping, even at low temperatures. Times of 10^{-4} sec are many orders of magnitude greater than what might reasonably be expected from present day germanium at room temperature. Furthermore, there has never been any indication of a distribution of time constants in bulk germanium, which would be needed if one tried to build up a 1/f spectrum from elementary shot noise spectra.

All of this is in sharp contrast to the surface. There is now experimental evidence not only for long-time processes at the surface, but for a distribution of time constants as well. In the next section an outline of the present picture of the germanium surface will be given.

Surface of Germanium

It is now well established that at the surface of germanium there are localized electronic levels with energies in the "forbidden" region between the valence and conduction bands. Charge residing in such "surface states", or in adsorbed ions (which will also be considered as surface states), is neutralized by a space charge region extending into the germanium to a depth of 10^{-4} to 10^{-6} cm. The resulting double layer may produce a sizable equilibrium difference in potential between the surface of the germanium and the bulk, as illustrated in Fig. 1-1. By a suitable choice of the gaseous ambient, it is possible to make the surface either strongly n- or p-type, irrespective of the bulk conductivity type. The space-charge region is conveniently described in terms of the parameters ϕ_B and ϕ_s, which are, respectively, the bulk and surface values of $(E_F - E_i)$. As usual E_F is the Fermi level and E_i is the energy corresponding to the Fermi level for intrinsic material (approximately the center of the gap). These quantities

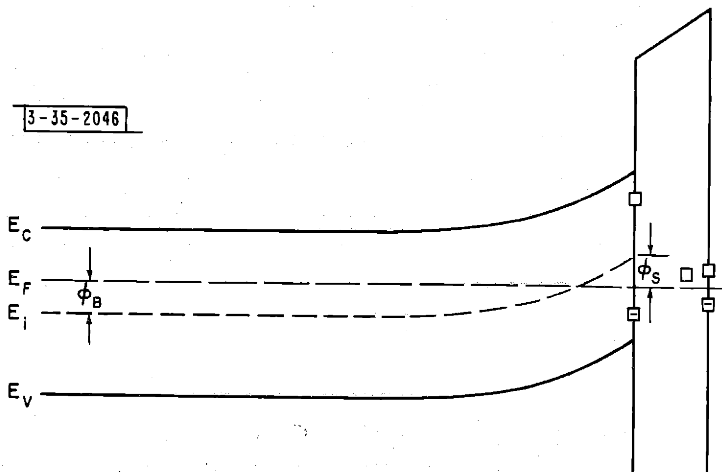

Fig. 1-1. Energy level diagram at germanium surface.

are shown in Fig. 1-1. There is normally a thin oxide layer on the surface of germanium, which has been indicated in the energy diagram by a potential barrier. The scale is greatly exaggerated, however, since the film is usually 20 to 50 Å thick.

The existence of surface states and space charge regions at the free surface of a semiconductor was proposed some time ago by Bardeen[25] to explain certain anomalies in metal-semiconductor rectification. More direct evidence for surface states was provided shortly afterward by an experiment of Shockley and Pearson,[26] in which they attempted to modulate the conductivity of a thin evaporated film of germanium by applying an external electric field normal to the surface. Since the change in the conductivity was only about 10 per cent of what had been expected from the magnitude of the induced charge and the free carrier mobility, it was necessary to assume that there were localized levels at the surface which could absorb and thereby immobilize the majority

of the induced charge. The existence of the space charge layer was later established by the work of Brattain and Bardeen[27] on the variation of contact potential with gaseous ambient and light. These experiments, in conjunction with measurements of the surface recombination velocity, led Brattain and Bardeen to propose that there were two sets of surface states at the germanium-germanium oxide interface, one near the conduction band and the other near the valence band.

Recent experiments on the modulation of surface conductivity of single crystal germanium by external fields,[28-32] together with measurements of surface conductance on junction transistor structures,[33-36] have now provided a much more detailed picture of the surface. These experiments indicate that there are two distinct classes of surface states in germanium. The first type is chiefly responsible for the high rate of recombination of holes and electrons at the surface, and probably consists of two or more levels in the manner suggested by Brattain and Bardeen. The other type of states have relaxation times of the order of seconds and minutes and, as we will show in the next chapter, possess a distribution of time constants. They are distinguished from the recombination states by these long times and by the strong dependence of their density and energy on the gaseous ambient. Because of the long time constants of these states, it would be almost impossible for them to be located at the germanium-germanium oxide interface. A much more plausible assumption is that they are either localized levels in the oxide layer or ions adsorbed onto the outer surface of the oxide. These slow states appear to be primarily responsible for the experimentally observed clamping of ϕ_S at a position which is a critical function of the surface history and environment, but which is practically independent of the bulk resistivity or the

presence of external or internal fields. Their density must be greater than $10^{13}/cm^2$ to account for such action.[25]

The density of the recombination states, on the other hand, seems to be much less than the original estimate of $10^{14}/cm^2$ made by Brattain and Bardeen.[25] Evidence has been found[36] for one set of states located about 0.15 ev below the center of the energy gap with a density of around $10^{11}/cm^2$, and it appears that there are states above the center of the gap with a density of the same order of magnitude.[31] The physical origin of the recombination states is not known, and as a result it is not clear whether their density and energy can be affected by the gaseous ambient.

Very little is known about the oxide layer which forms on an etched germanium surface. The stoichiometric composition has not been determined, nor is it known whether the film is amorphous or polycrystalline. Using electron diffraction techniques, R. D. Heidenreich, as quoted by Brattain and Bardeen,[27] found a film thickness of less than 10 Å immediately after a CP-4 etch, and a thickness between 20 and 50 Å after the surface had aged. By measuring the amount of oxide which is dissolved off in water, Green[37] has arrived at similar estimates. Fortunately it will not be necessary to probe too deeply into these matters here; the existence of the film and a rough idea of its thickness will be sufficient for our purposes.

Proposed Model for 1/f Noise in Germanium Filaments

This thesis will be concerned primarily with some of the effects produced by the slow surface states. In particular it will be proposed that 1/f noise is caused by a fluctuation in the charge of these states. Although the detailed quantitative arguments will be presented in Chapter II, we will now describe qualitatively how the 1/f noise could arise.

The slow states, or traps as they will often be called for brevity, can actually produce conductivity fluctuations in the germanium in two distinct ways. In order to see this, let us focus our attention on a small region of space surrounding one trap and ask how the concentration of holes and electrons in that region changes with time. Since the shot noise produced by the motion of the individual carriers is not being considered here, the rapid fluctuations in concentration due to carriers simply wandering through the region may be smoothed out by suitable short-term averaging. What we are interested in is the long-term, quasi-equilibrium change in concentration which occurs when one of these wandering carriers becomes trapped and remains in the region for a long time in the form of a localized, immobile charge. If a majority carrier is trapped, it is quite apparent that the (short-term) average number of free majority carriers in the region is reduced by almost one to preserve charge neutrality (a fraction of the charge is neutralized by a small average increase in free minority carrier concentration). If a minority carrier is trapped, it might be thought at first that the average number of free minority carriers in the region would be reduced by almost one. This is not the case, however. The trapped minority carrier is simply a localized charge, and like any other charge will be neutralized mainly by majority carriers. The number of minority carriers will decrease only slightly, while the average number of majority carriers will increase by nearly one. Therefore, whether the trapped carrier is a hole or electron, the conductivity of the region will change by an amount corresponding to the gain or loss of approximately one majority carrier, and the change will persist for the duration of the trapping. This is the first type of conductivity modulation that will be considered. For a further discussion of trapping, the reader is referred to papers by Fan[38] and by Haynes and Hornbeck.[39]

Unfortunately, the change in majority carrier concentration cannot account for the correlation effects observed by Montgomery;[9] the conductivity of each small region of the surface would fluctuate independently of the other regions. However, there is a second effect which can come about through the behavior of the minority carriers. The preceding discussion indicated that their concentration will change slightly when a hole or electron was trapped. If no voltage is applied to the sample, the magnitude of the change will be such as to maintain the thermal equilibrium p-n product. But with a field present, the minority carriers will be swept down the sample, and as a result their concentration in the vicinity of the trap will be returned to substantially the (thermal) equilibrium value. Therefore, the average p-n product will be changed. Hence, if recombination centers exist within the affected region, the recombination rate will be altered, while the generation rate will remain constant. The region can then act as a net source or sink for hole-electron pairs as long as the trap remains charged. This injection or extraction process will produce a change in the conductivity of the sample which is correlated over approximately a life-path for the minority carriers. Thus the interaction between traps and surface recombination states can give another type of conductivity fluctuation which would account for Montgomery's results. As will be shown in Chapter III, the two processes are of competing orders of magnitude. Except for the correlation experiment, there would not be any reason to emphasize one over the other.

While the injection extraction process described above is similar in some ways to Shockley's model, and was indeed suggested by his theory, it differs in two important respects. First of all, there are no further

assumptions introduced about the surface other than the existence of both recombination states and slow states or traps, for which there is now direct experimental evidence. Shockley's model, on the other hand, required the additional existence of certain crystalline imperfections. Although such imperfections were undoubtedly present in germanium samples several years ago, it is unlikely that they exist today. In fact this is probably the reason why present germanium filaments appear to be less noisy than is indicated by Montgomery's original measurements. It could well be that Shockley's mechanism, or something similar to it, was then operative (though not with his method for obtaining the long time constants) and produced an additional amount of noise.

The second difference is somewhat complicated and will be taken up in more detail in Chapter V. Briefly it is this. In Shockley's model the noise was obtained by a modulation of the generation rate of recombination centers in a fixed region. If the minority carrier concentration were reduced to zero, then the maximum amount of noise would be produced. In the above theory just the opposite would happen. The noise is obtained in this case by a fluctuation in the p-n product, which produces a corresponding fluctuation in the recombination rate; but the generation rate is assumed to remain fixed. Hence if the p-n product were reduced to zero along the surface, an average current would be obtained; but there would be no fluctuations in this current other than shot noise. The experiments discussed in Chapter V seem to favor such a situation.

Actually the generation rate will change if $\phi_s > |E_t - E_i|$, where E_t is the energy level of the recombination centers. Since $E_t - E_i$ appears to be from 0.15 to 0.2 ev, this condition would only be met for a rather strongly n- or p-type surface. For such surfaces, the slow traps can produce

a third type of noise by modulating the generation rate of the recombination centers, as proposed by Shockley. These matters will be discussed later.

In Chapter III it will be shown that with a single trapping time τ for free carriers, both the modulation of the majority carrier concentration and the injection-extraction mechanism lead to a shot noise spectrum of the form $\tau/[1 + (\omega\tau)^2]$. To obtain a 1/f spectrum we need a $1/\tau$ distribution for these time constants. The experiments to be described in the next chapter have given evidence for just this distribution.

CHAPTER II

RELAXATION TIME OF SURFACE STATES IN GERMANIUM

The original experiments of Shockley and Pearson[26] on the modulation of surface conductivity of germanium by external electric fields are difficult to interpret since they were performed on polycrystalline evaporated films. As mentioned in Chapter I, this "field effect" experiment has recently been studied in more detail on single crystal germanium by several investigators.[28-32] This work has shown that when a voltage is suddenly applied to a parallel-plate condenser formed by a metal electrode and a thin slab of germanium, the conductance of the germanium is modified in a rather complex manner. First, a change corresponding to an induced charge of mobile majority carriers occurs within the RC charging time of the circuit. Then as the majority carriers, minority carriers, and surface recombination centers come to mutual equilibrium, the conductance increases or decreases (with a time constant of the order of the minority-carrier lifetime) to a new quasi-stable value. Finally, the conductance slowly decays back to practically its original equilibrium value, with a half-life for the decay ranging from a few milliseconds to several seconds depending on the surface treatment and the gaseous ambient. It is this last decay, and similar ones observed from inversion layers on transistors,[34-36] that require the existence of a second class of surface states.

The initial change in conductance and the transition to the quasi-stable state have been studied by Low,[29] while Brown and Montgomery[31,32] have used the quasi-stable value of the conductance as a means for determining the density of the surface recombination centers. We will not discuss this work further, since the primary interest here is in establishing a connection

between the slow states and 1/f noise. For this purpose an experimental investigation of the slow decay was carried out in cooperation with R. H. Kingston.[30] In the next section we will present some of the results of that study.

Experimental Study of the Relaxation Time

The samples used for the experiments were in the form of slabs, about 0.5 x 0.25 x 0.01 inches, cut from germanium which was nearly intrinsic at room temperature. Ohmic contacts were attached along the ends of the sample and a plane metal electrode was placed approximately 0.01 inches from the surface under study. The whole assembly was placed in a glass chamber which could be supplied with various gases and water vapor. The conductance measuring circuit was similar to that used by Low, except that it incorporated dc coupling and amplification for observation of the long-time relaxation effects.

Initial experiments were performed using a square-wave voltage on the electrode to determine the transient response. In addition to the unusually long times already discussed, it was observed that the decay was always non-exponential. One might suspect a non-linear phenomenon. However, with the exception of a near-intrinsic surface, the response was found not only to be symmetric with opposite field polarities but also to vary linearly with applied field. The non-linearity in the near-intrinsic case is to be expected since here the surface conductance is near its minimum value and will increase for a small induced charge of either sign.

On the basis of these observations it seemed apparent that the decay could be explained in terms of a set of traps having a distribution of time constants. While it is possible to analyze the relaxation transient as a sum

of simple exponentials, a more accurate method is to determine the amplitude of the conductance variation produced by applied sinusoidal electrode voltages. The relative response of the conductance as a function of the frequency of the driving signal will give the same information as an analysis of the transient. Data of this form were obtained by applying to the electrode a constant-amplitude sine wave, approximately 400 volts peak-to-peak, in the frequency range from 10^{-2} to 10^{3} cps. The system was found to be linear over this range of frequencies and also over a 10 to 1 change in amplitude.

The results for a typical run are shown in Fig. 2-1, in this case for a freshly-etched surface exposed to dry nitrogen, with the response normalized to unity at 1000 cps. To minimize minority-carrier injection effects, which can give a spurious high-frequency response, the back surface of the slab was sandblasted, thus reducing the lifetime to the order of 5 microseconds for the dimensions used. The dashed lines in the figure represent the response to be expected if all of the traps had the same time constant, corresponding to a simple exponential decay in the transient case. As expected from the transient behavior, the frequency response does not fit the curve for a single trapping time, but instead falls very gradually over many decades of frequency, still continuing in this case at 10^{-2} cps. Similar frequency curves were taken after various surface treatments. It was known from the transient behavior that the relaxation time was a critical function of gaseous ambient and surface history. Exposing a freshly etched sample to oxygen or air for several hours, for example, would always increase the decay time quite markedly. Also, for both a freshly-etched surface and a well-oxidized surface, wet nitrogen produces a more rapid relaxation than dry nitrogen. The effect of the water vapor is actually strong enough to

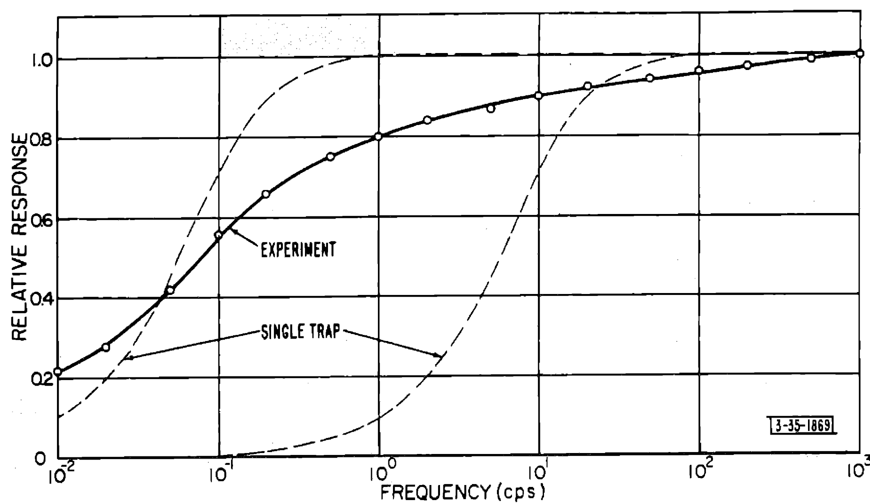

Fig. 2-1. Relative frequency response of surface conductance taken in dry nitrogen before oxidation.

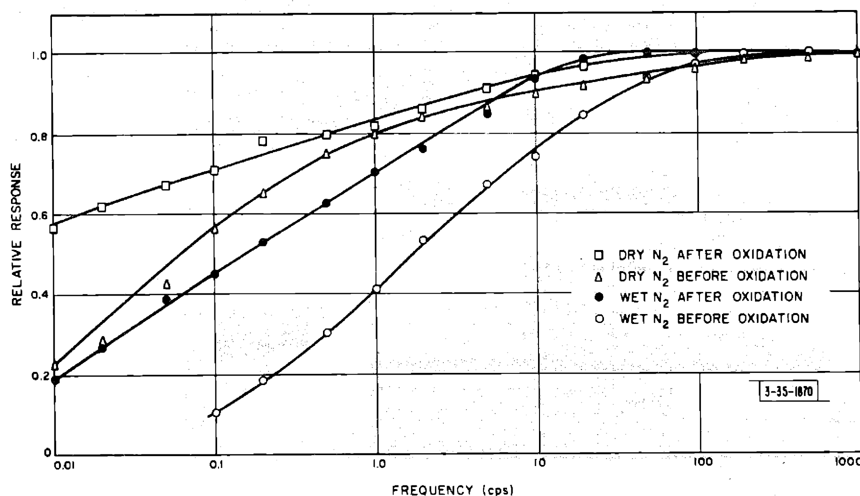

Fig. 2-2. Relative frequency response of surface conductance for several surface treatments.

counteract the effect of the oxidation: the decay for an oxidized surface in wet nitrogen is faster than for a freshly-etched surface in dry nitrogen. Typical frequency response curves for these cases are shown in Fig. 2-2. The "before oxidation" curves could not be obtained until approximately one-half hour after etching, since the surface was relatively unstable during the initial period and the steady drift in conductance made low-frequency measurements impossible. By observation of the transient response, however, it was found that during this period the time constant increased from a small value, of the order of several milliseconds, to a value in the 0.1 second range when the surface became stable enough to measure. The terms "before oxidation" and "after oxidation" should only be taken to mean before and after exposure to oxygen. At the present time the chemical behavior of a surface after etching and exposure to oxygen is not well understood. However, a general change in surface properties with time has also been observed in measurements of contact potential[27] and surface conductance;[34] and, as mentioned in Chapter I, the surface film does appear to thicken.

A few measurements made in a vacuum of 0.1 mm Hg indicated that the decay rate did not differ markedly from that in dry nitrogen, but the results are only qualitative. A better understanding of the chemistry of the surface is necessary before any quantitative data would be meaningful.

Even more interesting, especially from the standpoint of the noise theory to be presented later, is the fact that measurements made in nitrogen at temperatures close to that of liquid nitrogen actually showed a faster decay than at room temperature. This last result must be considered somewhat tentative because the role of bulk trapping[38,39] in these experiments is not completely known. Since illumination had no strong effect on the behavior,

it is believed that the observations are valid. In any case, as observed both in this work and by Kingston[34] on n-p-n junction structures, there is no appreciable change in the relaxation time for a wet surface between room temperature and -25°C.

Analysis

The slow time constants observed in these experiments are a measure of the rate at which electrons are transferred between the bulk and the states in, or on, the oxide layer. For the sake of discussion, consider the decay of excess electrons from the bulk into the surface states (the reverse rate may be shown to be equivalent by detailed balancing arguments). The limiting process for this decay could be either the transition rate of an electron to existing states, as in a normal trapping process, or the rate of creation of new levels. We must consider the latter as a possibility, since new states may be created either by the physical adsorption of additional molecules or by a chemical reaction between species present on the surface.

However, adsorption as the rate-limiting process can be ruled out at once because the time constants are not strongly pressure dependent. It should be mentioned that the decay in photoconductivity of ZnO after the removal of the light is remarkably similar in appearance to the decays observed here, and that for the ZnO this transient has been explained in terms of an adsorption-desorption process.[40] But since the decay in ZnO is definitely non-linear (the rate varies with the light intensity), it is not related to the strictly linear process found here.

The temperature independence of the decay, on the other hand, makes it almost impossible for a chemical reaction to be the determining factor. Certainly any reaction involving water can be eliminated, even without the

liquid nitrogen data, since there is no marked change as the temperature is lowered far past the freezing point.

Thus an electronic transition to existing levels seems to be the only reasonable explanation for the long time constants. We will not have to assume anything more about the physical processes involved. The rest of the analysis for the field-effect experiment, and the calculation for the 1/f noise, can be made without recourse to a more specific model. At the end of the next chapter, however, we will show that a tunneling process for the electron transfer can easily account for both the relative temperature independence and the required distribution of time constants.

The following discussion will be confined to frequencies which are low compared with the reciprocal of the lifetime, so that we may always assume that the majority carriers, minority carriers, and surface recombination centers are in mutual equilibrium. The recombination states can then be ignored in trying to explain the frequency response curve for the conductance variation. In the frequency range under consideration they simply absorb a fixed percentage of the added free carriers, an effect equivalent to changing the scale factor for the conductance variation.

We will first consider the case where all of the traps have the same characteristics. The form of the frequency response can of course be obtained directly from the transient behavior, but the object of the analysis will be to get an explicit relation for the time constants in terms of the other parameters of the system.

In addition to the usual notation, the following symbols will frequently be used:

n_s, p_s = concentration (no./cm^3) of electrons and holes, respectively, at the surface

N_t = concentration (no./cm^2) of traps

n_t, p_t = concentration (no./cm^2) of full and empty traps, respectively.

E_t = effective energy level of the traps

c_n = probability per unit time that an electron is captured by an empty trap

c_p = probability per unit time that a hole is captured by a full trap

Then the net rate in increase of electrons in the traps will be

$$\frac{dn_t}{dt} = \left(n_s p_t c_n - n_t N_c c_n e^{-\frac{E_c - E_t}{kT}}\right) - \left(p_s n_t c_p - p_t N_v c_p e^{-\frac{E_t - E_v}{kT}}\right), \qquad (2.1)$$

where the usual step of going through a detailed balancing argument has been omitted. For a justification of (2.1), the reader is referred to the treatment of recombination statistics by Shockley and Read.[41] Denoting the equilibrium values by n_{so}, p_{so}, etc., and the deviations from equilibrium by δn_s, δp_s, etc., we obtain for the linearized form of (2.1)

$$\frac{d\delta n_t}{dt} = p_{to} c_n \delta n_s - n_{to} c_p \delta p_s - \left[c_n(n_{so} + n_{s1}) + c_p(p_{so} + p_{s1})\right] \delta n_t$$
$$+ n_{to} N_c c_n e^{-\frac{E_c - E_t}{kT}} \delta\left(\frac{E_c - E_t}{kT}\right) + p_{to} N_v c_p e^{-\frac{E_t - E_v}{kT}} \delta\left(\frac{E_c - E_t}{kT}\right), \qquad (2.2)$$

where in notation similar to reference (41)

$$n_{s1} = N_c e^{-\frac{E_c - E_t}{kT}}$$
$$p_{s1} = N_v e^{-\frac{E_t - E_v}{kT}} . \qquad (2.3)$$

The terms involving $\delta(E_c - E_t)$ comes in for traps located outside of the germanium-germanium oxide interface since the presence of an applied field can then change the value of $(E_c - E_t)$.

We will often need the relation between δn_s and the total increase in electrons/cm^2 in the conduction band, which we may denote by δN, together with an analogous relation between δp_s and the increase of holes/cm^2 in the

valence band, denoted by δP. For this purpose it is convenient to define two quantities, N_o and P_o, by

$$\begin{aligned} \delta N/N_o &= \delta n_s/n_{so} \\ \delta P/P_o &= \delta p_s/p_{so} . \end{aligned} \qquad (2.4)$$

For the linear case we have been dealing with, it is shown in Appendix B that

$$\begin{aligned} N_o &= -\frac{kT}{qE_{so}}(n_{so}-n_o) \\ P_o &= \frac{kT}{qE_{so}}(p_{so}-p_o), \end{aligned} \qquad (2.5a)$$

where E_{so} is the equilibrium field at the surface with positive direction outward, and p_o and n_o are the equilibrium bulk concentration of holes and electrons, respectively. If there is no surface space charge and $E_{so} = 0$, then (2.5a) takes the form

$$\begin{aligned} N_o &= n_o\sqrt{\frac{kT\kappa\varepsilon_o}{q^2(n_o+p_o)}} = L_D n_o \\ P_o &= p_o\sqrt{\frac{kT\kappa\varepsilon_o}{q^2(n_o+p_o)}} = L_D p_o , \end{aligned} \qquad (2.5b)$$

where

$$L_D = \sqrt{\frac{kT\kappa\varepsilon_o}{q^2(n_o+p_o)}} . \qquad (2.6)$$

We will refer to L_D as the Debye length, although it differs by a factor $\left[(n_o+p_o)/2n_i\right]^{1/2}$ from the definition used by Shockley.[42] If the germanium is nearly intrinsic, as was the case for the field effect measurements, then for either an n- or p-type surface

$$N_o + P_o \simeq (n_{so}+p_{so})\sqrt{\frac{kT\kappa\varepsilon_o}{q^2(n_{so}+p_{so})}} = (n_{so}+p_{so})L_{Ds} , \qquad (2.7)$$

where L_{Ds} is the Debye length computed from the surface concentrations.

We will first use these results to show that the terms involving $\delta(E_c - E_t)$ in (2.2) may be neglected to a first approximation. For consider the ratio of the first and fourth terms on the right hand side of (2.2):

$$\frac{p_{to} c_n \delta n_s}{n_{to} c_n N_c e^{-\frac{E_c-E_t}{kT}} \delta\left(\frac{E_c-E_t}{kT}\right)} = \frac{\delta n_s}{e^{-\frac{E_t-E_F}{kT}} N_c e^{-\frac{E_c-E_t}{kT}} \delta\left(\frac{E_c-E_t}{kT}\right)} \qquad (2.8)$$

$$= \frac{\delta n_s/n_{so}}{\delta\left(\frac{E_c-E_t}{kT}\right)} .$$

Let E be the field in the oxide and w be the thickness of the oxide layer. Then from (2.4) and (2.7), assuming the dielectric constant of the oxide is about the same as that of the bulk germanium,

$$\frac{\delta n_s/n_{so}}{\delta\left(\frac{E_c-E_t}{kT}\right)} \simeq \frac{K\epsilon_0 E/q(N_0+P_0)}{q w E/kT} = \frac{K\epsilon_0 kT}{q^2(N_0+P_0)} \frac{1}{w} \simeq \frac{L_{Ds}}{w} \qquad (2.9)$$

for nearly intrinsic germanium. Since L_{Ds} 500 Å for the gaseous ambients used and w 50 Å, the ratio is greater than 10. Similarly, the second term in (2.2) is more than ten times greater than the fifth.

With sinusoidal ($e^{j\omega t}$) excitation and the above simplifications, equation (2.2) becomes

$$j\omega \delta n_t = p_{to} c_n \delta n_s - n_{to} c_p \delta p_s - \left[c_n(n_{so}+n_{s1}) + c_p(p_{so}+p_{s1})\right] \delta n_t , \qquad (2.10)$$

where as usual the factor $e^{j\omega t}$ has been omitted from all terms. If the capacitance between the electrode and the germanium is C f/cm^2 and the applied voltage is δV, then the charge induced in the germanium is

$$\delta Q = q(\delta P - \delta N - \delta n_t) = C\delta V. \qquad (2.11)$$

From the assumption that the majority and minority carriers are in equilibrium at the frequencies of interest,

$$\delta n_s/n_{so} = -\delta p_s/p_{so} . \qquad (2.12)$$

Substituting (2.10) and (2.12) into (2.11) and using the definition of N_o and P_o from (2.4), we obtain

$$\frac{C\delta V}{q} = -(N_o+P_o)\frac{\delta n_s}{n_{so}} - \frac{p_{to}c_n n_{so} + n_{to}c_p p_{so}}{c_n(n_{so}+n_{s1}) + c_p(p_{so}+p_{s1}) + j\omega}\,\frac{\delta n_s}{n_{so}}, \tag{2.13}$$

or solving for n_s/n_{so},

$$\frac{\delta n_s}{n_{so}} = -\frac{C\delta V}{q}\,\frac{c_n(n_{so}+n_{s1}) + c_p(p_{so}+p_{s1}) + j\omega}{(j\omega+N_o+P_o)\left[c_n(n_{so}+n_{s1})+c_p(p_{so}+p_{s1})\right] + c_n p_{to}n_{so} + c_p p_{so}n_{to}}. \tag{2.14}$$

If we define

$$\tau = \frac{N_o+P_o}{(N_o+P_o)[c_n(n_{so}+n_{s1}) + c_p(p_{so}+p_{s1}) + c_n p_{to}n_{so} + c_p p_{so}n_{to}}, \tag{2.15}$$

then we may rewrite (2.14) in the form

$$\frac{\delta n_s}{n_{so}} = -\frac{C\delta V}{q}\,\frac{1}{N_o+P_o}\,\frac{F+j\omega\tau}{1+j\omega\tau}, \tag{2.16}$$

where

$$F = \frac{(N_o+P_o)\left[c_n(n_{so}+n_{s1}) + c_p(p_{so}+p_{s1})\right]}{(N_o+P_o)[c_n(n_{so}+n_{s1}) + c_p(p_{so}+p_{s1}) + c_n p_{to}n_{so} + c_p p_{so}n_{to}}. \tag{2.17}$$

To compute the actual value of the change conductance, one must know the extent to which the mobilities of the free carriers near the surface are reduced by the presence of a potential well, which exists whenever $\phi_B \neq \phi_s$. If we first assume that the well is shallow enough so that the mobilities are not appreciably altered, the change in surface conductivity, in mhos per square, is

$$\delta G = q\mu_n\,\delta N + q\mu_p\,\delta P = q\mu_n N_o\frac{\delta n_s}{n_{so}} + q\mu_p P_o\frac{\delta p_s}{p_{so}} \tag{2.18a}$$

$$= C\delta V\left(\frac{\mu_p P_o - \mu_n N_o}{N_o+P_o}\right)\frac{F+j\omega\tau}{1+j\omega\tau}.$$

For values of $(\phi_B - \phi_s)$ greater than a few kT/q, this approximation is not very good. Schrieffer[43] has recently computed the change in surface conductivity that would be produced in the field effect experiment if the charge in the surface states remained fixed, which would correspond in our case to frequencies such that $\omega \gg 1/\tau$. Following his notation, we may define a "field-effect mobility" by

$$\mu_{FE} \equiv \delta G/\delta Q \Big|_{\delta n_t = 0} = \delta G / C\delta V \Big|_{\delta n_t = 0} , \tag{2.19}$$

which takes into account the change both in the number of carriers and in the surface mobility. Then at lower frequencies, where $n_t \neq 0$,

$$\delta G = C\delta V \mu_{FE} \frac{F + j\omega\tau}{1 + j\omega\tau} . \tag{2.18b}$$

Schrieffer has given a curve of μ_{FE} vs ϕ_s for intrinsic germanium, but in this chapter we will not need the numerical values. The ratio of δG at very low frequencies to that at very high frequencies is just F. Experimentally, this ratio is always found to be very small, so $F \ll 1$. But from (2.17) this means that

$$\left[c_n(n_{so}+n_{s1}) + c_p(p_{so}+p_{s1})\right](N_o + P_o) \ll c_n n_{so} p_{to} + c_p p_{so} n_{to} . \tag{2.20a}$$

Using the definitions of n_{s1} and p_{s1} from (2.3), this may be rewritten as

$$\frac{p_{to} n_{to}}{N_t} \gg N_o + P_o , \tag{2.20b}$$

which for nearly intrinsic germanium becomes

$$\frac{p_{to} n_{to}}{N_t} \gg (n_{so} + p_{so}) L_{Ds} \tag{2.21}$$

from (2.7). Loosely speaking, we may say that (2.21) requires that the number of both full and empty traps be large compared with the number of free carriers within a Debye length of the surface.

Inequality (2.20) could have been obtained more directly since $\frac{p_t n_t}{N_t} / (N_o + P_o)$ is just the ratio of δn_t to $(\delta N - \delta P)$ after equilibrium has

been reached between the traps and the conduction and valence bands. Since the transient response of the conductance to an applied field shows that practically all of the added carriers eventually become trapped, $\delta n_t/(\delta N - \delta P) \gg 1$ at equilibrium. To see what density of traps this requires, consider the case of a well-oxidized surface exposed to water vapor. Under these circumstances it has been found[34] that n_{so} is as large as $10^{17}/cm^3$. Since the frequency response still approaches zero at very low frequencies, condition (2.21) holds, giving

$$\frac{1}{4} N_t \geq \frac{n_{to} p_{to}}{N_t} \gg 10^{11}/cm^2 . \qquad (2.22)$$

Therefore, for this particular case N_t must be at least $10^{13}/cm^2$. It is not unlikely that the water vapor produces a trap density as large as $10^{15}/cm^2$, or about one trap per surface atom. Even with dry ambients it is necessary to assume that $N_t > 10^{13}/cm^2$ to account for the clamping of ϕ_s.[25,34]

Returning now to equation (2.18), we obtain with $F \ll 1$

$$\delta G \simeq C \delta V \mu_{FE} \frac{j\omega\tau}{1 + j\omega\tau} , \qquad (2.23)$$

where τ can also be simplified to

$$\tau \simeq \frac{N_o + P_o}{n_{so} p_{to} c_n + p_{so} n_{to} c_p} . \qquad (2.24)$$

Equation (2.24) gives the time constant that would be observed in the transient response; or to put it more precisely, if an excess bulk charge $\delta Q_B = q(\delta P - \delta N)$ is added to the sample, then the rate at which δQ_B decays into the traps when $F \ll 1$ is

$$\frac{d\, \delta Q_B}{dt} = - \frac{\delta Q_B}{\tau} . \qquad (2.25)$$

It is important to note that the expression for τ no longer contains any term involving the depth of the traps. Essentially, τ is the capture time for free carriers near the surface; the time that the carrier remains in the trap does not enter into (2.24).

The conductance variation given by (2.23) is for the case where all of the traps have the same characteristics. It has already been shown in connection with Fig. 2-1 that it takes a distribution of time constants to explain the observed frequency response. Now in any very small region an electron has only one effective capture probability given by an average over all of the traps in that region. Hence, if we are to get a distribution of time constants, we must assume that there is a reasonably coarse-grained variation in the capture times of the traps from spot to spot along the surface. Regions of the order of a Debye length square (roughly 10^{-5}x 10^{-5}cm) are sufficiently grainy for this purpose since the conductance of a region that size can fluctuate independently of the rest of the surface.[42] Therefore, assuming that τ is essentially constant over such an area, we may divide up the surface into regions a Debye length square, compute the conductivity variation from each one by (2.23), and then superimpose the results with an appropriate distribution function for τ to get the total conductivity variation of the sample. The use of the statistical treatment in obtaining (2.23) is still valid since in any area of 10^{-10} cm^2 there will be at least 10^3 traps, and perhaps as many as 10^5.

We will now show that a $1/\tau$ distribution for the time constants is what is needed to explain the majority of the experimental curves. Suppose that such a distribution holds between a lower limit τ_1 and an upper limit τ_2. Then using (2.23) the relative frequency response or the system function will be

$$S(\omega) = \int_{\tau_1}^{\tau_2} \frac{1}{\tau} \frac{j\omega\tau}{1+j\omega\tau} d\tau \Big/ \int_{\tau_1}^{\tau_2} \frac{1}{\tau} d\tau = \frac{\ln \frac{1+j\omega\tau_1}{1+j\omega\tau_2}}{\ln(\tau_2/\tau_1)}, \qquad (2.26)$$

which in the intermediate range where $\omega\tau_1 \ll 1 \ll \omega\tau_2$ reduces to

$$S(\omega) = \ln \omega\tau_2 / \ln (\tau_2/\tau_1) . \tag{2.27}$$

As illustrated in Fig. 2-2, a logarithmic dependence on ω is the behavior usually observed. In the next chapter an approximate method for obtaining the noise spectrum from the system function will be given. There it will be shown that the curve of Fig. 2-2 taken in dry N_2 before oxidation corresponds to a $1/f^{1.25}$ power spectrum, while the others give the more common $1/f^{1.0}$ spectrum.

The rest of the discussion of the field effect experiment and its relation to the 1/f noise will be postponed until after the proposed noise model has been analyzed.

CHAPTER III

1/f NOISE IN GERMANIUM FILAMENTS

As we have shown in the last chapter, if the field effect experiment is analyzed on the premise that the rate limiting process is the electronic transition to the traps, then in order to obtain the observed frequency response curves one is forced to make two assumptions. The first is that the density of the traps is greater than about $10^{13}/cm^2$. (Actually this is already known from other experiments.) Then the conductivity change due to a single trap or a group of similar traps becomes proportional to $j\omega\tau/(1 + j\omega\tau)$, where τ is the average time that a carrier near the surface remains free. The second assumption is that this capture time τ varies from spot to spot along the surface and that the distribution of τ is approximately proportional to $1/\tau$ up to very long times, at least greater than 100 sec.

These two assumptions are all that is necessary to obtain a 1/f spectrum from the model presented in Chapter I. In fact this is all that is needed to make a quantitative prediction for the magnitude of the noise which is in agreement with the experimental values. Just as in the analysis of the field effect experiment, it will not be necessary to assume a specific energy level or density for the traps.

Equilibrium Conductivity Modulation

In order to keep the ideas as simple as possible to begin with, we will first neglect the interaction between the slow traps and the recombination centers. As we have previously mentioned, this interaction can produce an injection or extraction of hole-electron pairs when an electric field is applied. Later this more complicated effect will be considered; for the

present, however, we wish to calculate only the noise to be expected from the fluctuation in free carrier concentration produced by the filling and emptying of the slow traps.

If possible, one always tries to analyze such complex fluctuations as a sum of a large number of elementary processes which are independent of one another (or more precisely, uncorrelated), for then the total power spectrum can be obtained by simply adding up the spectra from the elementary processes. This approach fortunately can be followed in the present case, but the way in which to analyze the fluctuations is perhaps not immediately apparent.

We have seen from (2.21) that the number of traps must be large compared with the number of free carriers within roughly a Debye length of the surface. Hence, the filling and emptying of any one trap will certainly not be independent of the filling and emptying of every other trap. For if only a fraction of them become filled, nearly all of the free electrons are removed from the surface. Therefore, the chance that one of the remaining traps can also capture an electron is reduced almost to zero; whereas for the traps to be independent, the capture probability must remain constant.

On the other hand, one cannot treat each charge carrier as a particle which behaves independently of all of the other carriers and try to follow it through its various states; e.g., first free and drifting down the sample, then trapped, then free again, etc. For even forgetting the fact that quantum mechanics would usually forbid distinguishing one carrier from another, there is an objection from the statistical point of view simply because charged particles interact with one another. The probability that a particular electron is in some given region of space depends on how many other electrons are there. If a majority carrier drifts out of the sample

(or out of any other region for that matter), then within a dielectric relaxation time on the average it is replaced by another majority carrier.

A procedure which does prove to work, however, is to divide up the surface into small regions about a Debye length square, just as in the field effect analysis, and then compute the conductivity fluctuation from each region separately. Since the conductivity fluctuations will be substantially independent for areas of this size, the total noise can be obtained by adding up the contribution from each region, with an appropriate averaging being taken over the different time constants.

It is shown in Appendix C that if S is the area of the elementary regions, then the power spectrum for the fluctuation of $\delta S n_t = S(\delta P - \delta N)$ is

$$G(\omega) = S(N_o + P_o) \frac{4\tau}{1+(\omega\tau)^2} , \tag{3.1}$$

where N_o and P_o are defined by (2.5) and τ by (2.24). This is exactly the result that would be obtained from the shot-noise fluctuation in the concentration of a group of independent particles, where the average concentration was $S(N_o + P_o)$ and each particle had the same lifetime .

In Appendix B it is shown that to a linear approximation one additional in the traps changes the number of electrons in the conduction band by

$$\int \delta N \, da = - \frac{N_o}{N_o + P_o} \tag{3.2a}$$

and the number of holes by

$$\int \delta P \, da = \frac{P_o}{N_o + P_o} , \tag{3.2b}$$

where the integration is over the surface. Suppose first that $(\phi_B - \phi_s)$ is small enough to allow the use of bulk mobilities for carriers near the surface. Then if a dc voltage V_o is applied to the sample of length L, each additional electron produces a current $q\mu_n V_o/L^2$ and each additional hole a current $q\mu_p V_o/L^2$. Hence the spectrum for the current fluctuation due to the one

region under consideration is approximately

$$G_{I_s}(\omega) = \left(\frac{qV_o}{L^2}\right)^2 \left(\frac{P_o\mu_p - N_o\mu_n}{N_o + P_o}\right)^2 S(N_o+P_o)\,\frac{4\tau}{1+(\omega\tau)^2}\,. \qquad (3.3a)$$

When $(\phi_B - \phi_s)$ is larger than a few kT/q, the correct expression for the spectrum is

$$G_{I_s}(\omega) = \left(\frac{qV_o}{L^2}\right)^2 \mu_{FE}^2\; S(N_o+P_o)\,\frac{4\tau}{1+(\omega\tau)^2}\,, \qquad (3.3b)$$

where μ_{FE} is defined by (2.19). (The change in the bulk conductivity is the same whether ϕ_s is changed by an applied field or by a trapped charge.)

If we now assume a $1/\tau$ distribution for τ between a lower limit τ_1 and an upper limit τ_2, then the total power spectrum for the current fluctuation is

$$G_I(\omega) = \frac{LC}{\ln(\tau_2/\tau_1)}\left(\frac{qV_o}{L^2}\right)^2 \mu_{FE}^2\,(N_o+P_o)\,\frac{4}{\omega}\left(\tan^{-1}\omega\tau_2 - \tan^{-1}\omega\tau_1\right), \qquad (3.4)$$

where C is the circumference of the filament. In the frequency range where $\omega\tau_1 \ll 1 \ll \omega\tau_2$,

$$G_I(\omega) = \frac{LC}{\ln(\tau_2/\tau_1)}\left(\frac{qV_o}{L^2}\right)^2 \mu_{FE}^2\,(N_o+P_o)\,\frac{1}{f} \qquad \text{amp}^2/\text{cycle}\,. \qquad (3.5)$$

It should be noted that the only parameters needed to specify the noise magnitude are the dimensions of the sample, the value of ϕ_B and ϕ_s, and the ratio τ_2/τ_1. The last quantity, which is known roughly from experimental observations, is not at all critical since it enters logarithmically. The quantity $(N_o + P_o)$ can be expressed in terms of ϕ_B and ϕ_s through (2.5a) and the expression for E_{so} given in Appendix B, while from Schrieffer's[43] formulas it would be possible to compute μ_{FE} for arbitrary values of ϕ_B and ϕ_s. For the special case of $\phi_B = 0$, Schrieffer has already calculated μ_{FE}. We have used his values to plot $q^2\mu_{FE}^2(N_o + P_o)$ vs ϕ_s in Fig. 3-1. Although

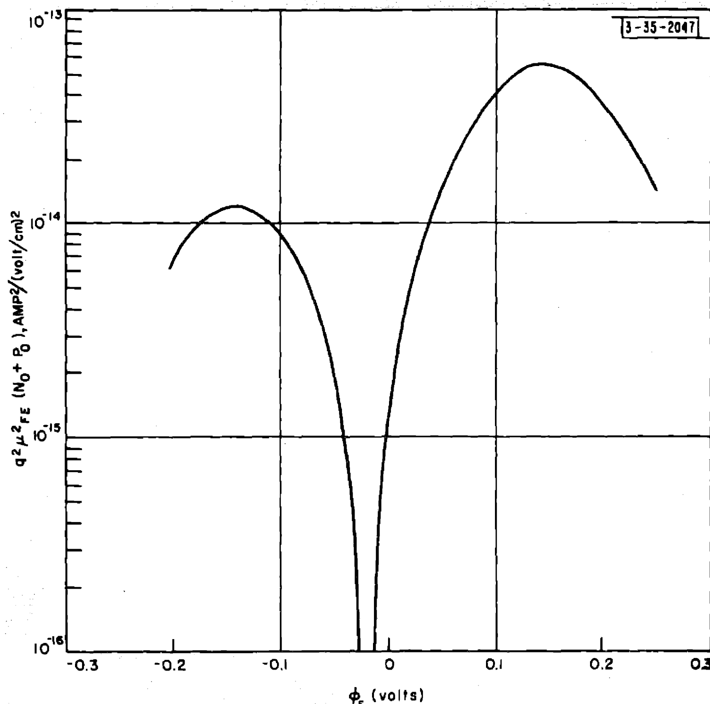

Fig. 3-1. Values of $q^2\mu_{FE}(N_o + P_o)$ vs ϕ_s for intrinsic germanium.

(3.5) indicates that the noise vanishes when $\mu_{FE} = 0$ (approximately when $N_o\mu_n = P_o\mu_p$ for nearly intrinsic germanium), only a minimum would actually be expected since the surface is not completely uniform.

To see what order of magnitude (3.5) predicts for the noise, we will consider a specific numerical example. Suppose we take $\phi_b = 2\ kT/q \simeq 0.05$ ev and $\phi_s = 4\ kT/q \simeq 0.10$ ev. This corresponds to an n-type bulk resistivity of about 10 ohm-cm. Instead of giving absolute numbers, which would be difficult to interpret, we will give the ratio between the predicted 1/f noise and shot noise. The power spectrum for the shot noise current fluctuations in n-type germanium is[1]

$$P_o L A \left[\frac{q V_o}{L^2} (\mu_n + \mu_p) \right]^2 \frac{4 \tau_p}{1 + (\omega \tau_p)^2} , \qquad (3.6)$$

where P_o is the bulk concentration of holes, τ_p is the lifetime of the holes, and A is the cross sectional area of the filament.

For the example chosen, with $(\phi_B - \phi_s)$ only 2 kT/q, μ_{FE} may be approximated by

$$\mu_{FE} \simeq \frac{P_o \mu_p - N_o \mu_n}{P_o + N_o} \simeq -\mu_n$$

without much error. Also the approximate expression (2.6) is accurate enough for the calculation of $(N_o + P_o)$. This gives $(N_o + P_o) \simeq N_o \simeq 2 \times 10^{10}/\mathrm{cm}^2$. We will further assume a filament about 0.05 x 0.05 cm in cross section, a lifetime τ_p of about 10^{-5} sec for these dimensions, and $\tau_2/\tau_1 \sim 10^8$. If for this last quantity either 10^4 or 10^{16} were taken, the final answer would be changed only by a factor of 2. For frequencies such that $\omega \ll 1/\tau_p$, we then obtain

$$\frac{N_{1/f}}{N_{shot}} = \frac{\frac{LC}{\ln(\tau_2/\tau_1)} \left(\frac{q V_o}{L^2}\right)^2 \mu_{FE}^2 (N_o + P_o) \frac{1}{f}}{LA \left(\frac{q V_o}{L^2}\right) (\mu_n + \mu_p)^2 P_o 4 \tau_p} \qquad (3.7)$$

$$= \frac{1}{4 \ln(\tau_2/\tau_1)} \frac{C}{A} \left(\frac{\mu_n}{\mu_n + \mu_p}\right)^2 \frac{N_o}{P_o} \frac{1}{\tau_p f}$$

$$= \frac{1}{4(20)} \frac{4(.05)}{(.05)^2} \left(\frac{3600}{3600 + 1700}\right)^2 \frac{2 \times 10^{10}}{3 \times 10^{12}} \frac{10^5}{f}$$

$$= \frac{300}{f}$$

Hence the 1/f noise would be equal to shot noise at about 300 cps under these conditions. With different values of ϕ_s the magnitude of the 1/f noise could vary by a factor of ten or more either way. Recent measurements on good single crystal germanium[23,44] have indicated that the frequency at which the 1/f noise equals the shot noise is usually between 200 and 2000 cps, which is in agreement with the value predicted by (3.7).

Injection-Extraction Type of Conductivity Modulation

While the simplified model presented thus far gives the right order of magnitude for the 1/f noise, it completely fails to account for the correlation effects observed by Montgomery.[9] As discussed in Chapter I, such a correlation can be obtained when the interaction between the traps and the recombination centers is considered. What has been tacitly assumed in the previous calculation is that when a voltage is applied to the sample in order to measure the 1/f resistance fluctuations, no disturbance is made in the carrier concentrations. This is a very good approximation for the majority carriers at the surface since their concentration is primarily determined by the necessity of neutralizing the charge in the traps. But the fluctuation of the minority carrier concentration in a given region is not determined by the trap occupancy of that region. These carriers are being constantly swept "downstream" by the applied field and replaced by ones coming from "upstream". If in some region the quasi-equilibrium state produced by a given trap occupancy is such that the majority carrier concentration is low and the minority concentration high, then when a longitudinal field is applied, this region loses its excess minority carriers but retains its low majority carrier density. (The region loses as many majority carriers as minority, but the percentage change in the majority carrier density is negligible.)

Since the p-n product is now less than n_i^2, the recombination rate of hole-electron pairs via the recombination states is reduced, while the generation rate of these same centers remains constant. (We will assume that the surface is not so strongly n- or p-type that we need to consider a fluctuating generation rate, as mentioned in Chapter I.) Thus the recombination centers tend to restore the quasi-equilibrium state, with the result that the region acts as a net source for hole-electron pairs as long as the trap occupancy remains fixed. Conversely, a region which temporarily had a high majority carrier density would act as a net sink for hole-electron pairs. This situation was not considered in the field effect analysis because there the conductivity variation of the entire surface was in phase. Although any one region might tend to act as a net source or sink, the overall conductivity change due to the injection-extraction process cancels out.

Unfortunately, we have not been able to obtain a solution for the injection-extraction type of conductivity modulation in as general a form as the preceding one. There are two cases to consider, depending on whether the traps communicate primarily with the majority carriers or with the minority carriers. The first case is easy to handle, but the second presents a very complicated statistical problem that has not yet been solved.

To simplify the terminology, let us assume that the surface is n-type with holes as the minority carrier. Then if the traps communicate primarily with the conduction band, the calculation for the spectrum of the trap occupancy is unchanged to a first approximation, so that (3.1) may still be used. This is because the fluctuations will be produced mainly by electron transitions between the traps and the conduction band, and, as just discussed, the applied voltage does not appreciably affect the majority carrier concentration. Even more important, however, is the conclusion that the trap occupancy

in one region of the surface still fluctuates independently of the trap occupancy in any other region.

If we forget about fluctuations of the order of the minority carrier lifetime or faster, then the number of holes in the sample will be some function of the trap occupancy along the surface. (After a change in the trap occupancy, the hole concentration should reach a new quasi-equilibrium state in a time comparable with a lifetime.) If we divide the surface into regions of area S as before and denote the trap occupancy in region k by $Sn_t^{(k)}$ and the number of holes in the sample by P, then using a linear approximation, we may write for the slow fluctuation in P

$$\Delta P = \sum_k \left. \frac{\partial P}{\partial n_t^{(k)}} \right|_{\substack{\Delta n_t^{(m)} = 0 \\ \text{all } m}} \Delta S n_t^{(k)} \quad . \tag{3.8}$$

Now the number of excess holes in the sample due to generation from the region k is

$$g^{(k)} \tau_p^{(k)} = S r \left[n_i^2 - n_s^{(k)} p_s^{(k)} \right] \tau_p^{(k)} \ , \tag{3.9}$$

where r is the usual recombination coefficient and $\tau_p^{(k)}$ is the expected lifetime of the injected holes from region k. When $Sn_t^{(k)}$ changes by one electron, and the occupancy of the traps in the other regions is fixed, $p_s^{(k)}$ and $\tau_p^{(k)}$ do not change. The former is determined by the traps "upstream" and the latter by the traps "downstream". But $n_s^{(k)}$ will vary with $n_t^{(k)}$ and in approximately the way given by (B.21) in Appendix B. Using that relation we find that

$$\Delta P = \sum_k r p_{so} \tau_{po} \left(\frac{n_{so}}{N_o + P_o} \right) \Delta S n_t^{(k)} \ , \tag{3.10}$$

where τ_{po} is the lifetime when all of the $\Delta n_t^{(k)}$ are zero. Now if bulk generation is negligible compared with surface generation, as it usually is

in the thin filaments used for noise measurements, then $rn_i^2\tau_{po}C = A_{po}$, where as before C is the circumference of the filament, A is the cross sectional area, and p_o is the bulk equilibrium concentration of minority carriers. (We will assume that the bulk is also n-type.) Now each hole-electron pair will produce a current $(\mu_n + \mu_p)qV_o/L^2$ when a dc voltage V_o is applied. Therefore, the fluctuations in the current produced by the injection-extraction process will be

$$\Delta I = \frac{qV_o}{L^2}(\mu_n + \mu_p)\frac{Ap_o}{C}\frac{1}{N_o + P_o}\sum_k \Delta Sn_t^{(k)} . \tag{3.11}$$

This component of the current fluctuation must now be added to the one discussed in the last section. In the present case the $\Delta Sn_t^{(k)}$ fluctuate independently with a power spectrum still given by (3.1). When $Sn_t^{(k)}$ changes by one electron, then (3.11) gives for the change in ΔI due to the injection of hole-electron pairs

$$\frac{qV_o}{L^2}(\mu_n + \mu_p)\frac{Ap_o}{C}\Big/(N_o + P_o) , \tag{3.12}$$

while the discussion leading up to (3.3a) shows that the change in the majority carriers (here electrons) makes a contribution

$$-\frac{qV_o}{L^2}\mu_n , \tag{3.13}$$

assuming that $(\phi_B - \phi_S)$ is not too large. Hence (3.3a) becomes

$$G_I(\omega) = \left(\frac{qV_o}{L^2}\right)^2\left[\frac{(\mu_n + \mu_p)Ap_o/C}{N_o + P_o} - \mu_n\right]^2 S(N_o + P_o)\frac{4\tau}{1 + (\omega\tau)^2} . \tag{3.14}$$

After averaging over τ with the usual $1/\tau$ distribution, we obtain for a filament with an n-type bulk and surface

$$G_I(\omega) = \frac{LC}{\ln(\tau_2/\tau_1)}\left(\frac{qV_o}{L^2}\right)\left[\frac{(\mu_n + \mu_p)Ap_o/C}{N_o + P_o} - \mu_n\right](N_o + P_o)\frac{1}{f} \tag{3.15}$$

To compare the new component of noise with the old, we may use the same parameter values as before: $\phi_B = 0.05$ ev, $\phi_S = 0.10$ ev, and a filament 0.05 x 0.05 cm in cross section. Then the ratio of (3.12) to (3.13) is

$$\frac{(\mu_n+\mu_p)\frac{AP_o}{C}/(N_o+P_o)}{\mu_n} = \left(\frac{3600+1700}{1700}\right)\frac{(.05)(.05)}{4(.05)}\ \frac{3\times10^{12}}{2\times10^{10}} \simeq 3\ . \qquad (3.16)$$

Therefore, the injection-extraction process gives the same order of magnitude for the noise as does the simple modulation of the majority carrier concentration, and so would also agree with the experimental values. In the example chosen, Equation (3.15) would predict that the 1/f noise was equal to shot noise at about 1200 cps.

If we had assumed that the traps communicated primarily with the valence band instead of the conduction band, then nothing would be changed in the noise calculation up to (3.11). The charge in the traps would still be neutralized mainly by electrons in the conduction band and (3.10) would still hold for the quasi-equilibrium changes we are considering here. However, the procedure breaks down when we try to compute the power spectra for the $\Delta Sn_t^{(k)}$. Not only are they not given by (3.1), but they are no longer even independent of one another. The concentration of electrons in the traps now fluctuates from holes making transitions between the trap level and the valence band. The difficulty is that the concentration of holes in any one region is not determined by the trap occupancy of that region, but rather by the trap occupancy upstream. Hence the flow of minority carriers makes Δn_t in one region dependent on Δn_t in every other region. This is a far more complicated situation than the one just discussed, and no satisfactory solution has been obtained.

Relation between Noise Spectrum and Field-effect Frequency Response Curves

There are still some important matters which have not been discussed. First there is the question of what noise spectra would be predicted by the field-effect frequency response curves of Fig. 2-2. If $g(\tau)$ is the distribution function for τ, then from (2.23) we have for the system function

$$S(\omega) \propto \int_0^\infty g(\tau) \frac{j\omega\tau}{1+j\omega\tau} d\tau , \qquad (3.17)$$

and for the noise

$$N(\omega) \propto \int_0^\infty g(\tau) \frac{\tau}{1+(\omega\tau)^2} d\tau . \qquad (3.18)$$

It is apparent that $N(\omega)$ can be written directly in terms of the imaginary part of $S(\omega)$, but it was the magnitude of S which was actually measured in the experiments of Chapter II and S is almost entirely real in the frequency range of interest. While it is possible to go from the magnitude to the imaginary part by the use of Hilbert transforms, this procedure would give rather complicated expressions. A much easier, although approximate, way is as follows:

We first differentiate (3.17) with respect to ω, obtaining

$$S'(\omega) \propto \int_0^\infty g(\tau) \frac{j\tau}{(1+j\omega\tau)^2} d\tau . \qquad (3.19)$$

Since $g(\tau)$ is expected to be close to $1/\tau$ over a wide range, we may write $g(\tau) = f(\tau)\, 1/\tau$, where f will be some slowly varying function of τ between say τ_1 and τ_2 and will fall off outside of these limits (it must approach zero for very small or very large values of τ to make the integral of g equal to unity). Then

$$S'(\omega) \propto \int_0^\infty f(\tau) \frac{j}{(1+j\omega\tau)^2} d\tau . \qquad (3.20$$

Now the integrand $j/(1 + j\omega\tau)^2$ as a function of τ is almost constant up to $\tau = 1/\omega$ and then rapidly decreases as $1/\omega^2$ for larger τ. Furthermore,

$$\int_0^\infty \frac{j\,d\tau}{(1 + j\omega\tau)^2} = \frac{1}{\omega} . \tag{3.21}$$

Therefore, we may cut off the integration at $1/\omega$ in (3.20) and replace $j/(1 + j\omega\tau)^2$ by unity in this range without introducing much error for those ω such that $\omega\tau_1 \ll 1 \ll \omega\tau_2$. This gives

$$S'(\omega) \propto \int_0^{1/\omega} f(\tau)\,d\tau \qquad (\omega\tau_1 \ll 1 \ll \omega\tau_2) . \tag{3.22}$$

But from (3.18) we see that the arguments used for $S'(\omega)$ apply with only slight modification to $N(\omega)$. Hence we have approximately

$$N(\omega) \propto \int_0^{1/\omega} f(\tau)\,d\tau \qquad (\omega\tau_1 \ll 1 \ll \omega\tau_2) . \tag{3.23}$$

Therefore

$$N(\omega) \propto \frac{d}{d\omega} S(\omega), \tag{3.24}$$

which may be rewritten as

$$N(\omega) \propto \frac{1}{\omega} \frac{d}{d\ln\omega} S(\omega). \tag{3.25}$$

If $S(\omega)$ is proportional to $\ln\omega$, then as before we get $N(\omega) \propto 1/\omega$; otherwise the $1/\omega$ spectrum must be multiplied by a slowly varying factor. That it really is a slowly varying factor may be seen from Fig. 2-2, where the slope of the "worst" curve, as a function of $\ln\omega$, changes only by a factor of about 10 over five decades of frequency. In Fig. 3-2 we have plotted the values of $N(\omega)$ predicted by (3.25) for that $S(\omega)$. As can be seen, the points are roughly fitted by a curve varying as $1/f^{1.25}$ over the frequency range from 0.1 to 1000 cps. Such a $1/f^n$ law with n slightly greater than unity is of course quite often observed instead of the strict $1/f^{1.0}$ law. Thus we have the very encouraging result that the field effect measurements give experimental evidence for a time constant distribution corresponding to the

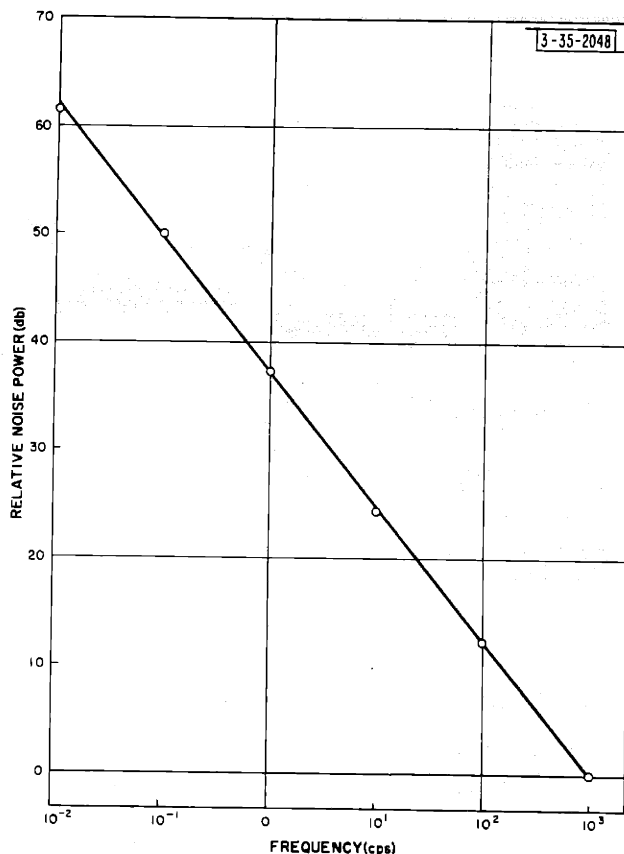

Fig. 3-2. Relative noise power predicted by "dry nitrogen--before oxidation" curve of Fig. 2-2.

general $1/f^n$ noise power spectrum.

The second point we wish to discuss cannot be disposed of so easily. It concerns the rather large values for τ_1 (the lower limit of the $1/\tau$ distribution) indicated by some of the curves of Fig. 2-2. It had been expected that the log f frequency response would continue to much higher frequencies, and it certainly would be much more pleasing from the standpoint of the 1/f noise theory if this were the case. However, there is not necessarily any disagreement between the curves of Fig. 2-2 and present

1/f noise measurements. As already mentioned, recent experiments on germanium filaments usually give a value between 200 and 2000 cps for the frequency at which 1/f noise equals shot noise. If a high frequency cutoff for the 1/f spectrum occurred in this region, it might easily be missed (the "cutoff" is not an abrupt break, but rather a gradual transition from a $1/f$ to a $1/f^2$ frequency dependence). Unfortunately, on some samples values of τ_1 as large as 0.01 sec have been found (e.g., the wet nitrogen curve after oxidation, Fig. 2-2); if the 1/f noise cutoff occurred at the same point, it should be quite unmistakable. On the other hand, values of τ_1 smaller than 10^{-4} sec have also been observed (e.g., the dry nitrogen curve before oxidation, Fig. 2-3), which could account for any of the high frequency noise measurements on filaments. The only way in which the question can be answered is by simultaneously measuring the 1/f noise and field effect on the same sample under a wide variety of surface treatments and gaseous ambients.

Such measurements will not be as easy to interpret as it might appear, however. It must be remembered that the preceding analyses for both the 1/f noise and the field effect were only valid for frequencies low compared with the reciprocal of the lifetime. From the field effect experiment it is known that very complicated minority carrier effects can set in at frequencies above a few hundred cycles, especially when the surface and bulk are of opposite types of conductivity. One of the clearest indications of this is that a decided difference is observed at higher frequencies between sand-blasting and etching the opposite face of the slab. It may well turn out that above a few hundred cycles the field effect experiment cannot be analyzed as simply as was done in Chapter II, or that there is another

process contributing to the 1/f noise which has been overlooked.

This discussion has been only for 1/f noise in germanium filaments. Of course it is well known that 1/f noise can exist up to a megacycle or more in junction diodes or point contact rectifiers. However, the physical structure and processes are completely different in these cases, and there would be no justification at all in extrapolating the upper frequency cutoff results of the field effect measurements on germanium slabs to such devices.

Possible Origin of $1/\tau$ Distribution

While the purely phenomenological treatment of the $1/\tau$ distribution which has been used up to now is sufficient for the noise calculations, it would be far more satisfying if some physical explanation could be given. The time constant measured in the field effect experiment and which occurs in the noise model is given by (2.24):

$$\tau = \frac{N_o + P_o}{c_n n_{so} p_{to} + c_p p_{so} n_{to}} . \tag{3.26}$$

To explain the frequency response curves of Chapter II, we must account for a range of these capture times from about 10^{-4} to 100 sec, and to explain 1/f noise the range must extend to at least 10^4 sec. Since n_{to} and p_{to} can only vary from about 10^{13} to $10^{15}/cm^2$, the range of capture times must come from a variation of c_n and c_p from spot to spot along the surface. This distribution must also be relatively temperature insensitive, both for the field effect and the 1/f noise.

To obtain an idea of the capture cross sections needed, let us assume $n_{to} \sim p_{to}$ and $c_n \sim c_p$. Then for an n-type surface

$$\tau = \frac{N_o}{n_{so} p_{to} c_n} . \tag{3.27}$$

Since $N_o/n_{so} \sim 10^{-5}$ cm and $p_{to} \sim 10^{14}/\text{cm}^2$, the capture cross section for electrons is

$$\sigma_n = \frac{c_n}{v} = \frac{1}{v} \frac{N_o}{n_{so} p_{to}} \frac{1}{\tau} \simeq \frac{1}{10^7} \frac{10^{-5}}{10^{14}} \frac{1}{\tau} = \frac{10^{-26}}{\tau} . \quad (3.28)$$

The capture cross section for holes, σ_p, would be of the same order of magnitude. For values of τ between 10^{-4} and 100 sec, σ_n and σ_p are between the order of 10^{-22} and 10^{-28} cm^2. It is obvious from these numbers that there must be a large potential barrier between the traps and the germanium surface, and hence that the traps are not located at the germanium-germanium oxide interface.

If the electrons were thermionically excited over the barrier, barrier heights greater than 0.5 ev would be needed to give the long time constants. But with such activation energies the decay in the field effect would be extremely temperature dependent, in contradiction to the experimental observations. Hence a thermionic emission process may be ruled out.

However, if the electrons tunnel through the barrier, we may get time constants as long as is needed, but with an inherently temperature independent process. Furthermore, we will show that tunneling can give a $1/\tau$ distribution in a completely natural manner.

It had first been thought that with a tunneling mechanism the electrons had to communicate with the traps in two steps: first a transition at constant energy from the conduction band to an excited level of the trap by tunneling, and then a transition from the excited level down to the ground level. Under these conditions there could have been no communication with the valence band, since by definition there would be no levels below the ground level to play a role analogous to the excited levels. However, Professor H. Brooks of Harvard has pointed out that this picture is not correct, and that a one-step

transition can be made from either band directly to the trap. Although a detailed analysis based on the correct model has not yet been carried out, it is possible to give a crude order-of-magnitude calculation for the transition probabilities.

If we again consider an n-type surface for convenience and assume that $c_n \sim c_p$ and $n_{to} \sim p_{to}$, then as before

$$\tau \simeq \frac{N_o}{n_{so} p_{to} c_n} \quad . \tag{3.29}$$

For a rectangular barrier of height V and width w, the wave functions of states in the conduction band are attenuated by an amount

$$e^{-\left(\frac{2mV}{\hbar^2}\right)^{\frac{1}{2}} w} \tag{3.30}$$

on the other side of the barrier. Hence the capture probability should be roughly

$$c_n = \sigma v e^{-2\left(\frac{2mV}{\hbar^2}\right)^{\frac{1}{2}} w} \tag{3.31}$$

where σ is of the same order of magnitude as normal trapping cross sections without barriers, say 10^{-13} to 10^{-15} cm^2. If we take V = 1 ev, w = 30 Å, $\sigma = 10^{-14}$ cm^2, v = 10^7 cm/sec, $N_o/n_{so} = 10^{-5}$ cm and $p_{to} = 10^{14}/\text{cm}^2$, then we find that $\tau \simeq 10$ sec. If w varies between 20 and 40 Å, then τ would vary from almost 10^{-4} sec to 10^5 sec.

In Chapter I we discussed the method of obtaining a $1/\tau$ distribution from a range of activation energies. Since the barrier width enters exponentially into the expression for τ in (3.31), we may obtain the same result by assuming a uniform distribution of barrier widths. To account for the observed values of τ, this distribution need only extend over a very small range, as was indicated by the calculation above. A uniform distribution would automatically be achieved if it were assumed that the traps were homogeneously distributed throughout the oxide layer. On the

other hand, if the traps arise from adsorbed ions, then a variation of the oxide thickness along the surface would give the desired distribution of barrier widths. As was mentioned in Chapter I, the oxide layer is estimated to be from 20 to 50 Å thick, which is just the right range for this model. Figure 2-2 shows how the time constants increase after exposure of a freshly-etched surface to oxygen. This could be explained in terms of a thickening of the oxide layer and hence the barrier width for tunneling.

In Chapter VI we will discuss the possibility of extending this tunneling mechanism to other sources of 1/f noise.

CHAPTER IV

CHANNELS AND EXCESS REVERSE CURRENT IN p-n JUNCTION DIODES

With the exception of the material in the last section, the work to be discussed in this chapter was performed in cooperation with R. H. Kingston. Although most of the experimental results have already been reported in the literature,[45] the general picture of reverse currents in p-n junction diodes has sufficiently improved since then to warrant a new presentation. In addition, some understanding of the excess current mechanisms in p-n junctions is necessary to interpret the noise measurements of Chapter V.

It is now clear that there are two distinct types of excess reverse currents in grown germanium p-n junctions. The first type is a leakage current which is induced by water vapor and which apparently flows through the oxide layer or on the surface of the oxide. It is characterized by the excess current being approximately linearly proportional to the applied reverse bias. For relative humidities above about 50 per cent and applied biases above 10 or 20 volts, this type is usually dominant. It was proposed by Law[46] that this leakage current is electrolytic. In support of that hypothesis he gave experimental data indicating that the reverse current began to increase at just the relative humidity when the adsorbed water was becoming mobile, that the number of ions required was in good agreement with the number present, and that the surface conductance as a function of the number of layers of adsorbed water was very similar to that obtained by other workers for quartz, where the leakage current is assumed to be ionic. More recent results make this explanation seem much less plausible. For if the current were ionic, one would expect either an evolution of gas

(hydrogen for the type of reaction considered by Law) or a transfer of mass from one side of the junction to the other. However, Law was not able to detect any hydrogen evolution; and Green,[37] in a very carefully controlled experiment, has obtained the same negative result. Furthermore, Green was also able to rule out a mass transfer process. These experiments suggest that the leakage current is electronic instead of ionic. If this is the case, then the slow states discussed in the preceding chapters may be producing the leakage: the current could be carried by electrons jumping from one trap to the next in a direction parallel to the surface.

Whenever the surface is made either strongly n- or p-type, a second type of excess current is produced which flows in a thin surface layer inside the germanium. For example, if the surface is n-type, then the n-type bulk region can be considered to extend out along the surface of the p-region. This effectively results in an increase in the area of the p-n junction and hence an increase in the reverse saturation current. Such surface layers with conductivity of opposite type from that of the bulk are known as "channels". They were first studied by Brown[47] on n-p-n transistors, where they form an ohmic leakage path between the emitter and collector. Christensen[48] later established the existence of channels on p-n junctions by observing the photoresponse of the units to a chopped-light source as the spot of light was moved from one end of the bar to the other. With no channel present, the photoresponse falls off exponentially on both sides of the junction; but when a channel exists, the response will remain approximately at its peak value for some distance on one side of the junction (as much as a millimeter or more) and then will fall off exponentially. In this way Christensen was able to investigate qualitatively the type and size

of channels produced by various surface treatments.

Since this optical technique allows the length of a channel (i.e., the distance over which the photoresponse remains approximately constant) to be determined as well as its existence, it provides a direct method for correlating the excess reverse current with the channel length. In the next section we will present some measurements for n-type channels produced by water vapor. These results show a direct proportionality between excess current and channel length up to about 10 volts of applied bias. This observation can be used together with experimental results on channel conductivity in n-p-n transistors to form a model of the channel behavior. The theory is complete enough to give a prediction for the excess current which is of the right order of magnitude and which has roughly the correct dependence on voltage and humidity. For biases greater than about ten volts the leakage current becomes appreciable, so that the total excess current is no longer proportional to the channel length.

Experimental Results for n-Type Channels

The experimental equipment was composed of three main parts: first, a sample chamber and associated apparatus for varying the humidity; second, a 900 cps chopped light source producing a line image 20 microns wide on the surface of the diode and parallel to the junction; and third, a 900 cps detector and dc bias and metering instruments. The last part needs no special comment, and the only unusual feature of the optical system was the inclusion of an infrared filter to limit the light penetration to about 10^{-4} cm. This ensured that all of the minority carriers generated by the light were collected by the channel rather than by the bulk junction. Humidity was controlled by circulating the ambient gas in a closed system

over different saturated salt solutions, thus obtaining the known vapor pressure associated with the particular salt.[49] This gave an easily reproducible set of relative humidities covering most of the range from 0 to 100 per cent. Furthermore, by a careful selection of the salts, nearly constant humidities could be obtained in the temperature range of 20 degrees to 30 degrees C.

There appears to be no channel present immediately following a CP-4 etch, and if the sample is very clean, no appreciable excess current in the low voltage region. However, exposure to wet oxygen for several hours will produce both large channels and excess currents, which agrees with the reported observations on n-p-n transistors.[34] This is probably the result of a thickening of the oxide layer; but as mentioned in connection with the field effect experiment, the chemical behavior of the surface during this period is not understood. In any event, prolonged exposure to wet oxygen finally results in a fairly stable surface. If the sample is then placed in nitrogen to minimize further possible changes, the surface is found to be nearly intrinsic at zero humidity and to become progressively more n-type as the humidity increases. The experimental results that will be presented next are for this type of surface preparation, which was the first one studied in detail. In the last section additional experimental results will be given for surfaces exposed to oxygen for shorter periods of time, which show p-type channels on the n-side in dry nitrogen. All of the quantitative results are for bars 0.20 x 0.20 x 2.0 cm cut from a grown germanium p-n junction having 1.6 ohm-cm p-type and 9 ohm-cm n-type resistivity, but the qualitative behavior has been reproduced on other samples.

For water-induced n-type channels on samples prepared as just described, a typical set of photoresponse curves is shown in Fig. 4-1. As can be seen, the end of the channel is somewhat indefinite. But if it is taken to be the point where the slope suddenly changes, as indicated by the vertical arrow, then for a range of applied reverse biases from 0.1 to 10 volts the excess current is found to be directly proportional to the channel length. Moreover, the constant of proportionality is independent of the relative humidity, as shown in Fig. 4-2. (The slope did increase slightly over a period of weeks, however.) Humidities below about 30 per cent produced channels too small to be measured by the light technique.

The excess reverse current vs voltage is plotted in Fig. 4-3 for several humidities. The theoretical curves also shown in this figure will be derived at the end of the next section.

Theory

By extending Brown's model[47] for channels in transistors to the p-n junction structure, a fairly complete picture of the channel behavior may be presented. As shown in Fig. 4-4, the channel essentially forms an extension of the normal reverse-biased junction area with an accompanying increase of current due to surface-generated holes being swept into the p-region and bulk-generated electrons swept into the channel. The electrons generated at the surface and those collected from the bulk combine to produce a longitudinal current in the channel which flows toward the n-side. The resulting voltage drop along the channel decreases the bias between the surface and the p-type material. Since a high field at the surface tends to pinch off the conduction path, the channel becomes wider as the distance from the junction increases. At large distances the width approaches the limiting value associated with

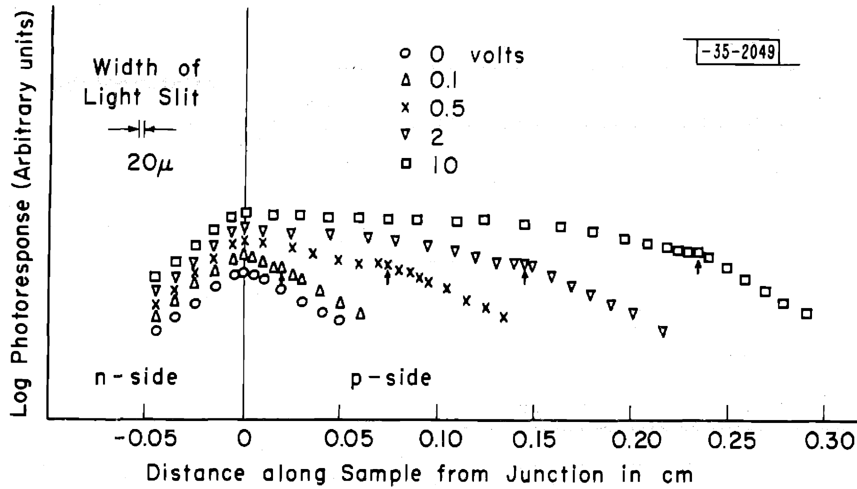

Fig. 4-1. Photoresponse curves at 100 per cent relative humidity, with the extent of the channel indicated by the vertical arrows. All curves were taken with a 10,000 ohm load resistor, but have been displaced vertically for clarity.

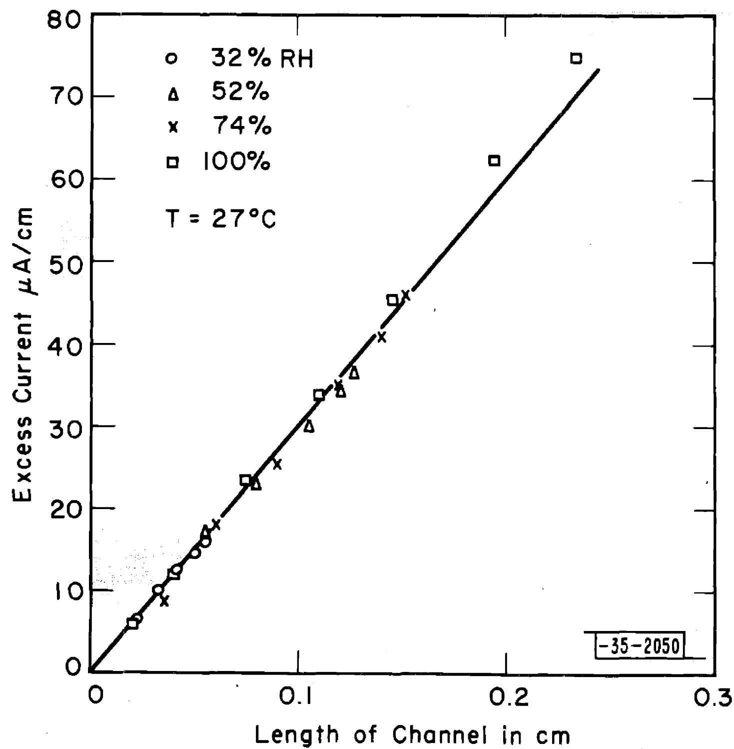

Fig. 4-2. Excess current per unit circumference vs channel length for several values of relative humidity.

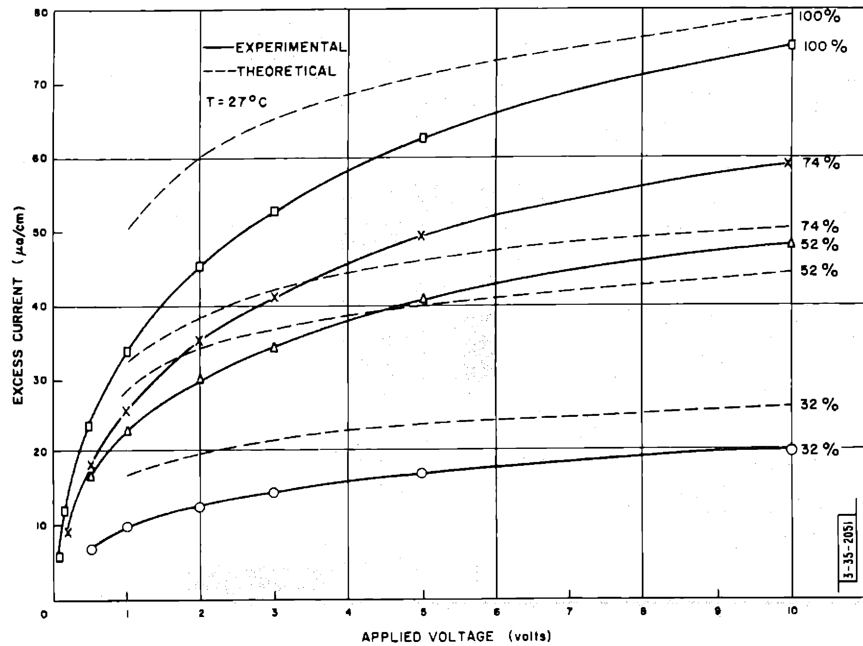

Fig. 4-3. Theoretical and experimental curves of excess current vs applied voltage.

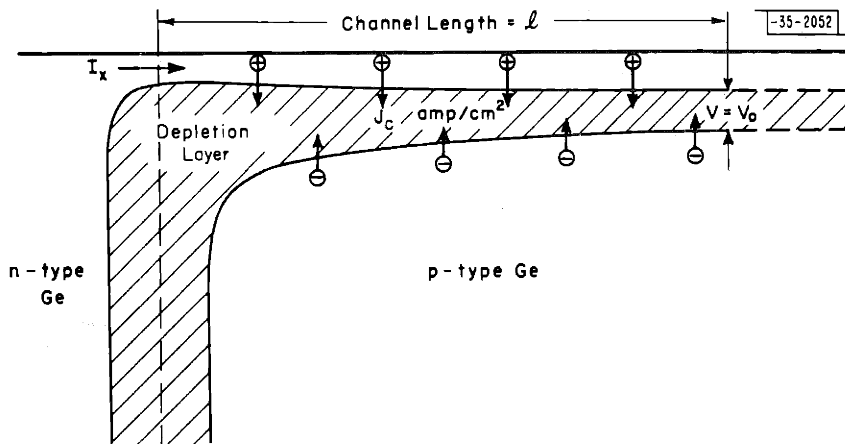

Fig. 4-4. Schematic diagram of channel showing the increase in the effective rectifying area of the diode produced by the n-type surface.

the equilibrium inversion region.[27] Thus in one sense the channel continues indefinitely, but only over the section for which the applied voltage is much greater than kT/q will the surface junction be acting as a perfect collector of minority carriers. As the applied bias drops through kT/q, there will be a rapid transition from full saturation current across the surface junction to the equilibrium condition of zero current, giving an effective length for the channel as far as excess current is concerned. Electrons generated further away than this from the junction must diffuse through the intervening distance in order to be collected, with the attending probability of recombining before the collection can take place. Thus a photoresponse curve would be expected to fall of exponentially beyond this effective end of the channel, indicating that ℓ is the length which is measured by the curves in Fig. 4-1.

Figure 4-2 shows that the saturation current J_c flowing across the surface junction is constant for this distance ℓ, which in turn implies that the surface generation is independent of the applied bais and the relative humidity, at least for humidities above 30 per cent. The slope of the curve gives a value for J_c of about 300 $\mu A/cm^2$. The part due to bulk generation can be calculated from the lifetime and is about 900 $\mu A/cm^2$, leaving a little over 200 $\mu A/cm^2$ to be attributed to generation at the surface.

It should be pointed out that Fig. 4-4 has been greatly distorted in order to show the whole channel region on one diagram. For the sample used in this experiment, the channel width is of the order of 10^{-6} cm, while the depletion layer between the channel and the p-region is about 10^{-4} cm, and that at the true junction is about 10^{-3} cm because of the small doping gradient. The width of the light slit is about twice that of the depletion layer.

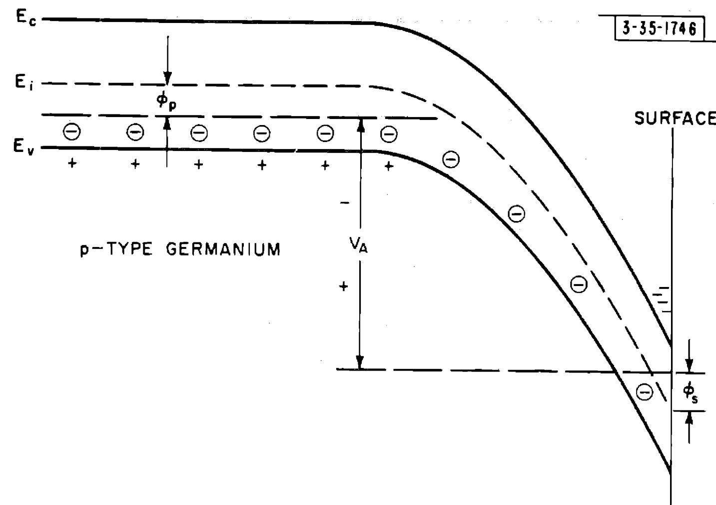

Fig. 4-5. Energy level diagram for n-type channel at surface of p-type germanium.

An energy band diagram of the channel is shown in Fig. 4-5. The electrostatic potential corresponding to the Fermi level for intrinsic material is denoted as usual by E_i; the deviation from E_i of the quasi-Fermi levels for holes in the bulk and electrons at the surface are given by ϕ_p and ϕ_s, respectively. By combining an approximate solution of Poisson's equation for this configuration with Schrieffer's[43] mobility calculation, Kingston[34] has obtained the following expression for the channel resistivity, valid for biases greater than about one volt:

$$R = \frac{2}{3}\left[\left(\frac{q}{kT}\right)^2 \frac{1}{K\epsilon_0} \frac{N_A}{n_i} \frac{\ell_s}{\mu_n} e^{-\frac{q\phi_s}{kT}}\right](V + \phi_p + \phi_s) \tag{4.1}$$

$$= A\,(V + \phi_p + \phi_s)\,.$$

where ℓ_s is the mean free path and μ_n is the bulk electron mobility. For smaller biases some of the approximations break down and a numerical

integration must be carried out. Using these calculations Kingston found that very good agreement could be obtained with the measurements of channel conductance on n-p-n transistors if he assumed ϕ_s to be a function only of the relative humidity and independent of the applied voltage. This behavior of ϕ_s is the same as that observed in the field effect experiment with external fields and can also be explained by the large density of the slow surface states. If the assumption of a constant ϕ_s is used here together with the observations of Fig. 4-2 on the proportionality of excess current to channel length, it is possible to derive an expression for the excess current in the p-n junction as a function of applied bias.

The previous discussion had shown that the longitudinal current flowing in the channel at a distance x from the junction is

$$I(x) = J_c(\ell - x). \tag{4.2}$$

Then if we use the approximate relation (4.1) we have

$$\frac{\partial V}{\partial x} = -RI = -A(V+\phi_p+\phi_s)\,J_c(\ell - x). \tag{4.3}$$

If the voltage at the end of the channel is denoted by V_o and the applied voltage by V_A, integration of (4.3) gives

$$\ln\frac{V_A+\phi_p+\phi_s}{V_o+\phi_p+\phi_s} = \frac{A J_c \ell^2}{2}. \tag{4.4}$$

Therefore the excess current is

$$I_x = CJ_c\ell = \left(\frac{2C^2 J_c}{A}\ln\frac{V_A+\phi_p+\phi_s}{V_o+\phi_p+\phi_s}\right)^{\frac{1}{2}}, \tag{4.5}$$

where C is the circumference of the sample.

The best experimental values for A for the surface treatment under consideration are given in Table I for several humidities. The values in the first column are those measured[34] on an n-p-n transistor with a p-type

TABLE I

Relative humidity	A n-p-n transistor	A p-n junction	ϕ_s
32 per cent	1.55×10^6 ohm/volt	3.2×10^6 ohm/volt	0.102 ev
43	0.69	1.4	0.121
58	0.50	1.03	0.129
75	0.41	0.84	0.133
88	0.30	0.62	0.140
100	0.165	0.34	0.152

resistivity of 3.3 ohm-cm. Since from (4.1) we have that A is directly proportional to N_A, the acceptor density, it is necessary to multiply these values by the ratio of the resistivities, 3.3/1.6, to obtain the appropriate values for the 1.6 ohm-cm material used here. These converted values are tabulated in the second column. In the third column are listed the corresponding values of ϕ_s computed from (4.1).

At this point all of the quantities in (4.5) are theoretically or experimentally known: V_o should be approximately $kT/q \simeq 0.026$ ev at room temperature; $\phi_p = 0.12$ ev from the p-type resistivity; ϕ_s and A, determined experimentally from an n-p-n transistor of similar surface treatment, are given in Table I; and J_c, determined experimentally from Fig. 4-2, is about 300 $\mu A/cm^2$. The excess current computed from these values is shown by the dashed lines in Fig. 4-3. As can be seen, the order of magnitude of the theoretical prediction is good, and the curves have the right general shape. The theoretical curves have not been continued below one volt since (4.5) is not valid for small biases.

Discussion

It is possible to achieve a better agreement between the theoretical and experimental curves of Fig. 4-3 if V_o is (4.5) is allowed to be an

adjustable parameter. A value of 0.5 volts for $(V_o + \phi_p + \phi_s)$ gives a fairly good fit for applied biases between one and ten volts. This was the procedure originally followed,[45] and it is not without justification since the model we have been using up to now is somewhat oversimplified. Actually it is only for the middle section of the channel that (4.2) is valid. At the far end the transition between full saturation current and zero current has been completely neglected. This includes both the decrease in J_c at very low voltages and the end effects that the channel produces on the diffusion flow pattern. Near the bulk junction, on the other hand, the problem really becomes two-dimensional because of the bending of the depletion layer. Furthermore, there is the added complication of the doping gradient in this region, for the transition from n-type to p-type material takes about 0.025 cm or more in the sample used. If the channel is long enough, that is if the applied voltage is high enough, then these end regions become relatively much less important, and in fact their effect becomes more like a modification of the boundary conditions for the middle section of the channel. Therefore it is not too unreasonable to try to lump all of these corrections into the one boundary parameter V_o and adjust that to give the best fit with experiment.

However, measurement of the channel lengths at higher voltages has since shown that the difficulty is more basic. Experimentally it has been observed that with applied biases up to 50 volts the channel length is more nearly proportional to the first power of ln $\left[(V_A + \phi_p + \phi_s)/(V_o + \phi_p + \phi_s)\right]$ than the square root of this quantity. Statz[50] has found such a logarithmic relationship to be approximately true even up to 120 volts for p-type channels produced by ozone. Since the excess current is still proportional to the channel length in this latter case, it is not (4.2) which is at fault.

Also the assumption that $_s$ remains constant seem to be valid even up to these high voltages[35] as would be expected if the density of the slow states is around $10^{14}/cm^2$. The trouble apparently lies in the expression for the channel resistance (4.1). It is easy to see that if we put

$$R = const. \frac{V + \phi_p + \phi_s}{\ln \frac{V + \phi_p + \phi_s}{V_0 + \phi_p + \phi_s}},$$

then a simple logarithmic dependence of the channel length on voltage would be obtained. At the present there is no theoretical justification for this, however.

One point which is of some interest is the independence of J_c on humidity. If the Shockley-Read theory[41] for traps is applied to the surface recombination states, it will be found that the net generation rate is

$$\frac{c_n c_p (n_i^2 - n_s p_s) N_t}{c_n(n_s + n_{s1}) + c_p(p_s + p_{s1})}, \qquad (4.6)$$

where c_n, c_p, n_{s1}, p_{s1}, and N_t are quantities analogous to those used in Chapter II, but defined for the surface recombination states instead of the slow traps. If there are two sets of recombination centers, another term must be added to (4.6). Since $p_s n_s$ will be zero for either n- or p-type channels, we have for the surface component of J_c

$$J_{cs} = \frac{q c_n c_p n_i^2 N_t}{c_n(n_s + n_{s1}) + c_p(p_s + p_{s1})} \qquad (4.7)$$

For the special case where $c_n = c_p$, Fig. 4-6 shows the dependence of J_{cs} on ϕ_s. The generation rate remains constant until $|\phi_s|$ becomes comparable with $|E_t - E_i|$ and then falls off exponentially for $|\phi_s| > |E_t - E_i|$. To explain the observed invariance of J_c, we must assume that we were operating on the flat portion of the curve. If $c_n = c_p$, this in turn would require that the recombination centers be located at least a few kT/q further from the center of the gap than the highest value of ϕ_s obtained, which was about 0.15 ev.

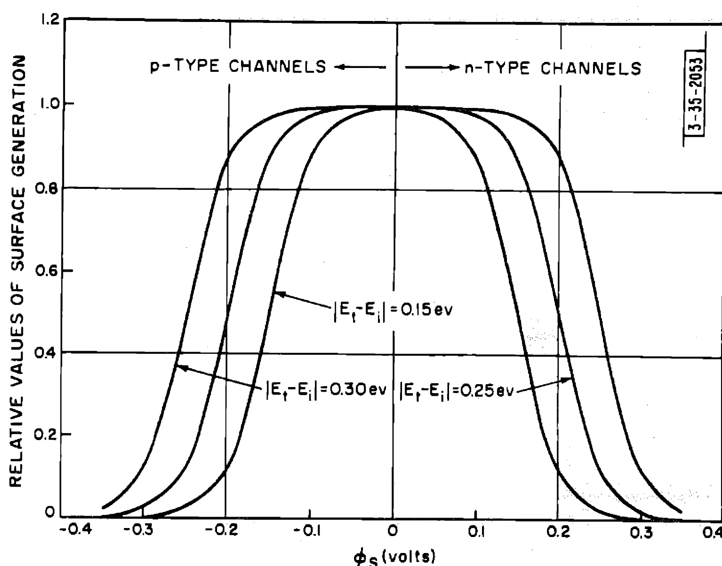

Fig. 4-6. Relative values of surface generation as a function of ϕ_s for n- and p-type channels.

It has recently been reported[36] that there is a set of recombination states located about 0.15 ev below the center of the gap with a density of the order of $10^{11}/cm^2$. Since this work was performed on p-type surfaces produced by ozone, it may not carry over to n-type surfaces produced by water vapor. If it does, however, then to reconcile our results with these we must assume either that $c_p > c_n$ or that another set of recombination centers is producing most of the generation.

Further Experimental Results

If a freshly-etched p-n junction is exposed to wet oxygen for only a few minutes instead of many hours and is then placed in a dry nitrogen ambient, it is possible to obtain a fairly stable p-type channel on the n-side of the

junction. These channels occuring in dry nitrogen show qualitatively the same behavior as the n-type channels induced by water vapor which we have just discussed. Water vapor will cause the p-type channels to diminish, and at a sufficiently high relative humidity, perhaps 50 per cent or more, they will finally vanish as the surface becomes intrinsic. At still higher humidities an n-type channel is formed on the p-side as before. Near the crossover point where there is a channel on neither side, the junction may exhibit excellent rectification characteristics.

Under these conditions the junction might be a far better rectifier in room atmosphere than in a dessicator, but it would not be stable. Further exposure to wet oxygen will cause the p-type channel to diminish and the n-type channel to increase, shifting the crossover point to a lower humidity. With a long enough exposure to wet oxygen we finally end up with the situation already discussed, where the surface is nearly intrinsic in dry nitrogen and strongly n-type in wet nitrogen. These same irreversible changes occur if the sample is kept in nitrogen, but then they take place rather gradually over a period of days or weeks instead of hours. Hence, an intermediate state of the surface may be obtained quickly with wet oxygen and then studied in a nitrogen ambient.

Figure 4-7 shows the reverse current of a p-n junction as a function of the relative humidity at four stages during this surface transformation. The reverse bias is 10 volts in all cases. It is interesting to note that the current at the crossover point, which is the saturation current without a channel, increases as the surface ages. This apparently is produced by a gradual increase in the surface generation rate.

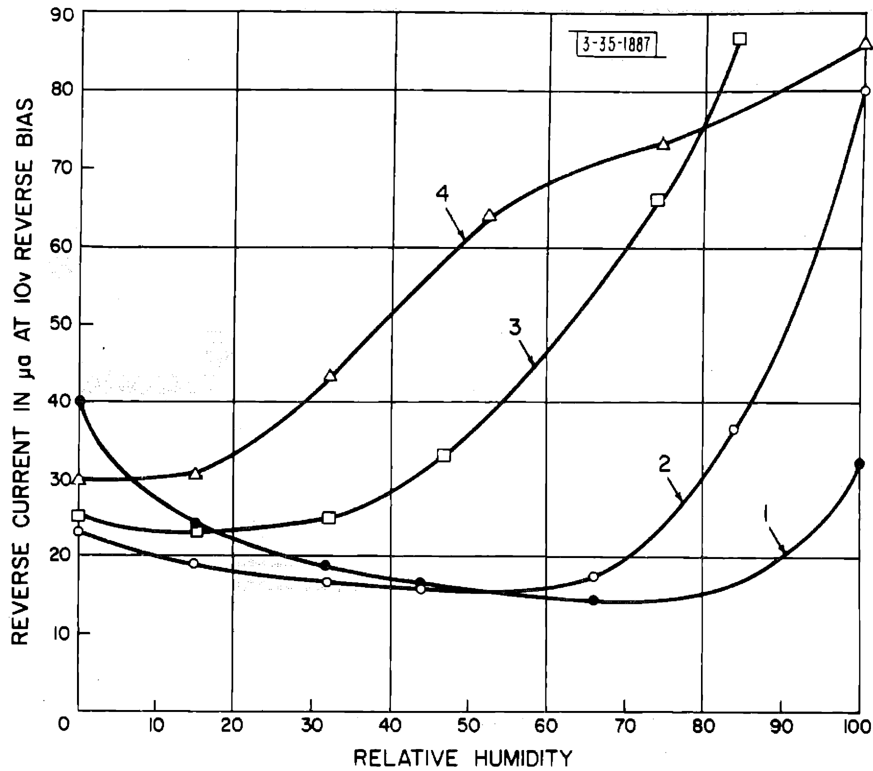

Fig. 4-7. Changes in reverse current vs relative humidity as surface becomes progressively more n-type from repeated exposure to wet oxygen.

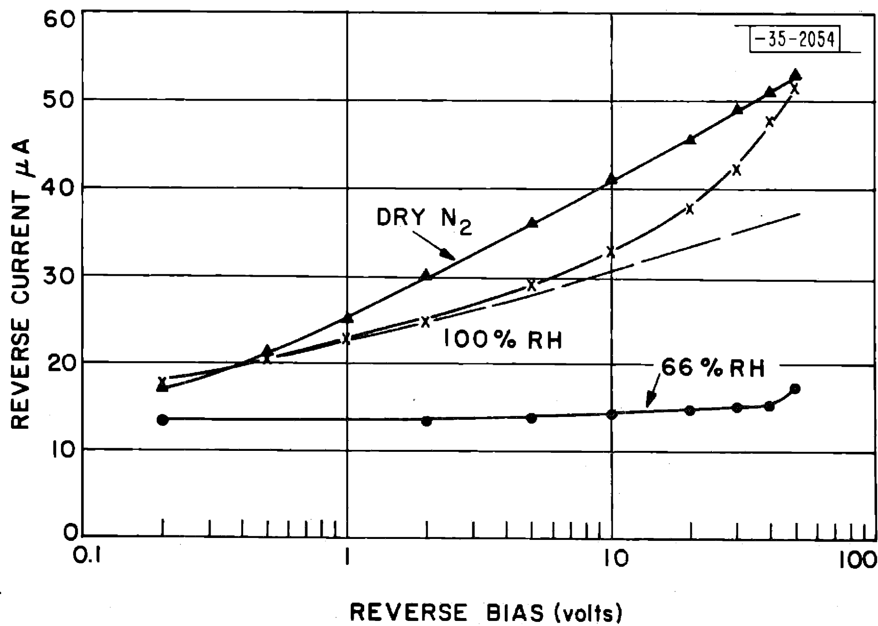

Fig. 4-8. Current-voltage curves for a reverse biased p-n junction, showing poor rectification characteristics at dry nitrogen and 100 per cent relative humidity, but good saturation at an intermediate humidity.

A representative set of current-voltage curves is presented in Fig. 4-8. At 66 per cent relative humidity the junction shows practically no excess current up to 30 v. and only 4 μA excess at 50 v. The curve for dry nitrogen exhibits a typical channel behavior--a nearly logarithmic dependence of the current on applied voltage. At 100 per cent relative humidity we see a combination of channel current and leakage current. The component of excess current due to the channel may be determined by a measurement of the channel length and is given by the dashed line. If this current is subtracted off, the remaining excess current increases linearly with the applied voltage. This is the behavior normally observed for the leakage current. A more accurate separation of the excess current into its two components up to even higher voltages has been done by Statz;[50] the above result is in agreement with his work.

It should be pointed out that the voltage-current characteristics thus far discussed are all taken under dc conditions. Both the channel and the leakage current show a transient behavior. A time of the order of a second is required for the channel to build up after the voltage is suddenly applied, and a further slow drift upward may be observed for several minutes. These times are the same as those observed in the field effect measurements of Chapter II and, according to the present model, arise from the same physical process, namely the transference of electrons between the bulk germanium and the slow surface states. A discussion of the channel transients, especially for n-p-n transistors, has been given by Kingston[34] and will not be repeated here.

The leakage current, on the other hand, typically shows an overshoot in current when the voltage is applied, followed by first a rapid fall and

then a more gradual decrease over a period of several minutes. The range of time constants is remarkably similar to that in the channel and the field effect and may be produced by the same electron transfer process. Law[46] has attributed this transient to a polarization effect; but as has been mentioned earlier, his interpretation of the leakage current as being electrolytic is in doubt.

CHAPTER V

1/f NOISE IN p-n JUNCTIONS

It is a well-known empirical observation that poor rectification characteristics and 1/f noise in p-n junctions usually go hand-in-hand. In fact the work described in the preceding chapter was undertaken because it was felt that an understanding of excess reverse currents was the key to the 1/f noise problem in p-n junctions. The experimental results which will be presented below have greatly strengthened this belief.

It has been found that there are two distinct types of 1/f noise produced in a reverse biased junction, which apparently correspond to the two types of excess current previously discussed. Since little is known about the leakage current, the noise associated with it can only be described experimentally. However, by combining the somewhat imperfect model of the channel presented in the last chapter with the noise theory of Chapter III, it has been possible to analyze two likely mechanisms for the production of noise in channels, namely fluctuations in the surface generation rate and fluctuations in the conductivity of the inversion layer. While neither mechanism leads to the correct voltage dependence, the calculation based on fluctuations in the channel conductivity will be shown to give the right order of magnitude for the noise associated with channels.

Experimental Procedure

All of the noise measurements to be presented in the next section were taken on the same diodes used for the channel measurements; i.e., on bars cut from a grown germanium junction with 9.0 ohm-cm n-type resistivity and 1.6 ohm-cm p-type resistivity. The surface treatment was also the same:

after a CP-4 etch, the samples were exposed to wet oxygen for varying amounts of time to obtain the desired surface condition and then were placed in a nitrogen ambient for greater stability while the noise measurements were being made.

It was decided to measure the short-circuit current noise as a function of dc voltage, rather than the open-circuit voltage noise as a function of the current. A resistance of 5 K was usually found to be an effective short circuit down to 0.2 v, even when channels were present. As a safety precaution, however, the noise was always checked for at least one other value of load resistance at the low voltages to make sure that the noise current was really independent of the load. Only wire-wound resistors were used, so that the noise from the load was only thermal and generally below even the flicker noise of the input stage (which was equivalent to about 10 K of thermal noise at 1 kc).

No precise measurements of the power spectrum were made, since the main interest was in the dependence of the noise on the surface condition and the applied voltage. However, spot checks at 100 cps, 1 kc, and 10 kc were frequently made during each run to be sure that the noise was really 1/f, while at other times a complete spectrum was taken from 100 cps to 40 kc. Except for data obtained at biases near 50 v at low humidities, the spectrum seemed to be given quite accurately over this range of frequencies by a constant term plus the 1/f component, which obeyed approximately a $1/f^{1.0}$ law.

Experimental Results

In a dry nitrogen ambient, where there is no leakage current, a sizable 1/f noise may be observed when a large p-type channel is present. If water

vapor is then added to the nitrogen, this noise decreases as the channel decreases, and at some intermediate humidity the diode may have both good rectification characteristics and also low noise. At still higher humidities, when the rectification characteristics begin to show the presence of a leakage current, a much larger 1/f noise with a different voltage dependence is found. This transition is shown rather clearly in Fig. 5-1 by the noise data corresponding to the voltage-current curves of Fig. 4-8, although better examples of noise associated with p-type channels will be given shortly. It should be noted that while the current was largest in dry nitrogen, the noise is largest at 100 per cent relative humidity, in fact some 25 db higher than for dry nitrogen when the bias is around 20 v. Within experimental error,

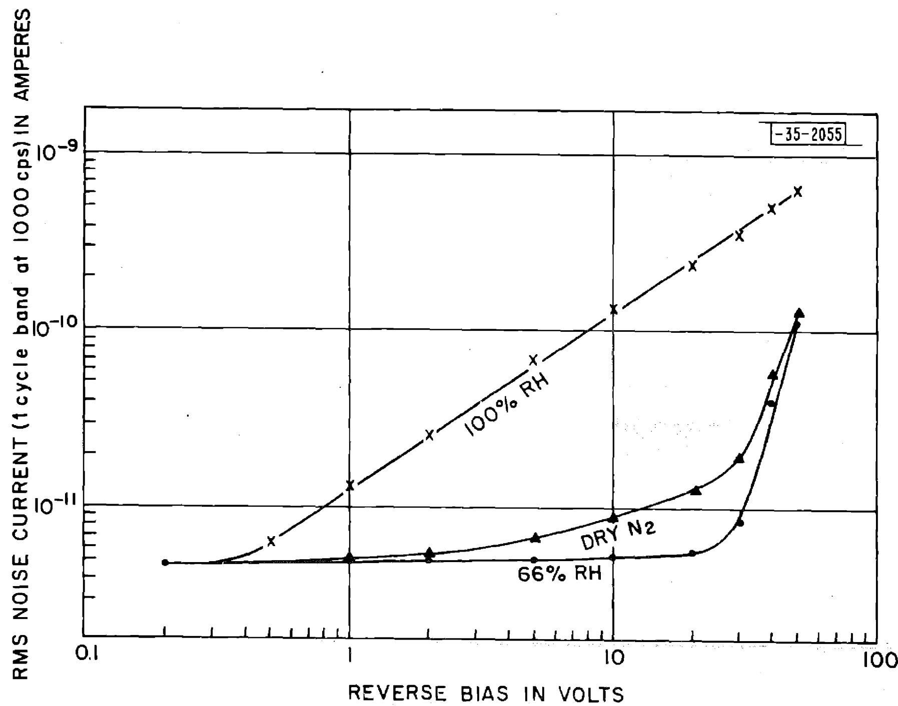

Fig. 5-1. Noise vs reverse bias for the p-n junction of Fig. 4-8.

the rms noise current at 100 per cent relative humidity increases in direct proportion to the voltage from 0.5 v to 50 v. This noise is apparently produced by the unknown leakage current. In Fig. 4-8 it was shown that the leakage current increases linearly with voltage and that it first becomes detectable around one volt. The linear increase of the rms noise current is just what would be expected if this noise is caused by fluctuations in the conductance of the leakage path; for if the average conductance is independent of voltage, the fluctuations in conductance would be expected to behave similarly, giving $\overline{\Delta i^2} = V^2 \, \overline{\Delta G^2} = \text{const.} \, V^2$. Although an n-type channel contributes most of the average excess reverse current at 100 per cent relative humidity, any noise due to the channel is apparently negligible in comparison with that arising from the leakage current. There is a small amount of noise due to the p-type channel, however, since the curve at 66 per cent relative humidity lies several db below the one taken in dry nitrogen.

The sharp increase of noise above 20 v for both dry nitrogen and 66 per cent relative humidity may be due to some form of breakdown. Above 30 volts a distinct change, which may be described as a kind of popping or spiky effect, could be seen in the broadband appearance of the noise on an oscilloscope. At the same time there was a large increase in the low-frequency noise components, which produced a marked deviation of the spectrum from a 1/f law. No attempt has been made to investigate this phenomenon in detail. However, it has been found that the effect is not particularly dependent on the surface conductivity or the relative humidity, which suggests that it is not connected with the surface at all.

Voltage-current characteristics are given in Fig. 5-2 for three p-type channels, all of which were produced on the same sample in dry nitrogen, but

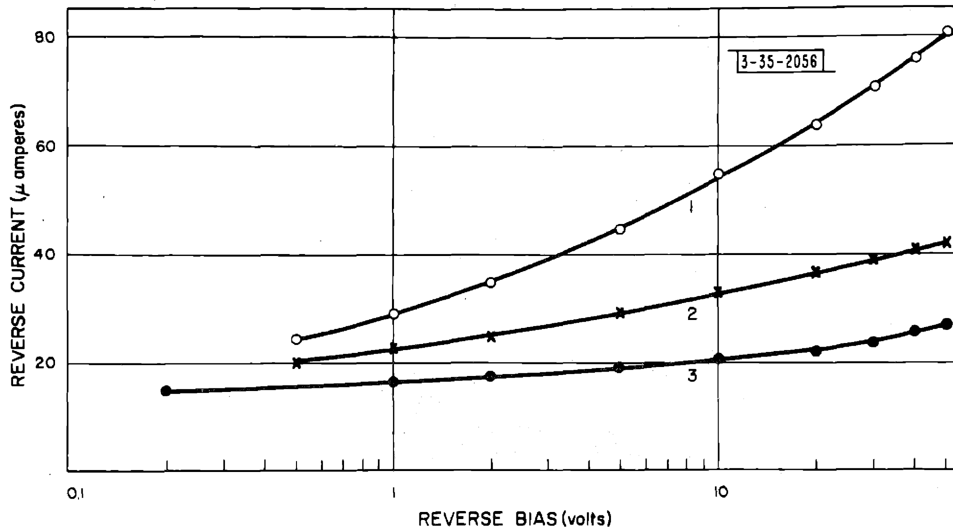

Fig. 5-2. Current-voltage characteristics for three p-type channels produced on the same sample in dry nitrogen, the decrease in the channel current resulting from repeated exposure of the surface to wet oxygen.

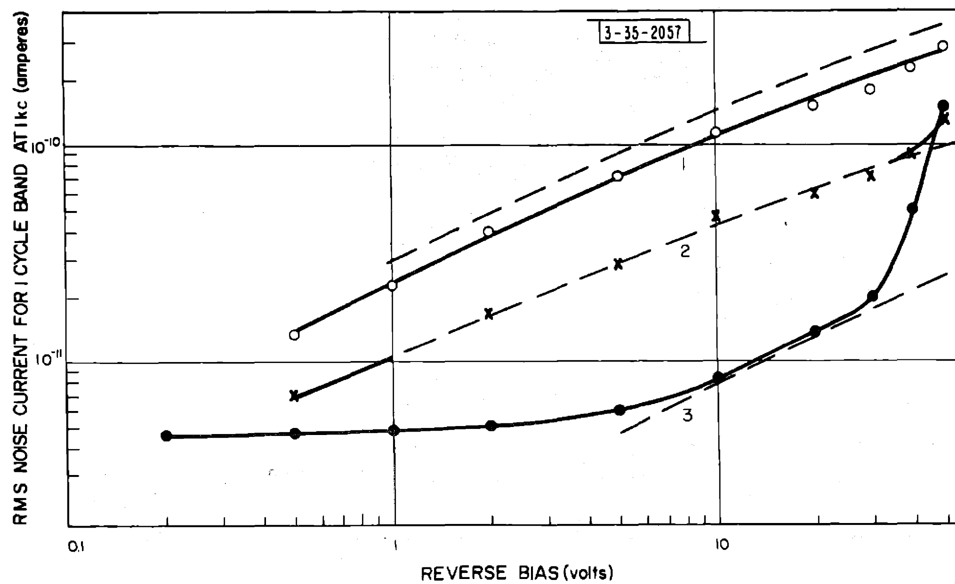

Fig. 5-3. Noise vs reverse bias corresponding to the curves of Fig. 5-2.

at different stages during the slow shift of the surface conductivity from p-type toward intrinsic. The corresponding 1/f noise measurements are shown in Fig. 5-3. It may be noted that the rms noise current associated with these channels does not increase linearly with the reverse bias, in contrast to the noise associated with the leakage current in Fig. 5-1. Also the noise in Fig. 5-3 does not increase logarithmically with voltage, as the channel current usually does. The sharp increase of the noise level above 30 v for the second and third curves is again associated with a change in the spectrum and a popping effect. The dashed lines shown in this figure, which were obtained from a semi-empirical formula, will be discussed in the last section.

Figure 5-4 shows the effect of varying amounts of water vapor on the 1/f noise from this junction. These measurements were made on the day that the third curve of Fig. 5-3 was taken. At each value of relative humidity the noise level remains fairly constant up to some critical voltage and then sharply increases by as much as 20 or 30 db for a slight additional bias. The critical voltage becomes smaller for higher humidities. Since the rms noise current increases linearly with voltage above this critical region, it is believed that the sharp rise is associated with the onset of the leakage current. This is also suggested by the current-voltage characteristics shown in Fig. 5-5. If these curves were replotted on a linear scale, they would be very nearly straight lines. The curves are given on the same logarithmic scale as the noise, however, to point out the interesting fact that there is no sudden increase in the reverse current at those voltages where the 1/f noise is increasing rapidly. Evidently the leakage current is so noisy that the fluctuations in it may be detected before the average value becomes appreciable. Some hysteresis effects were noticed in the critical voltage region, especially

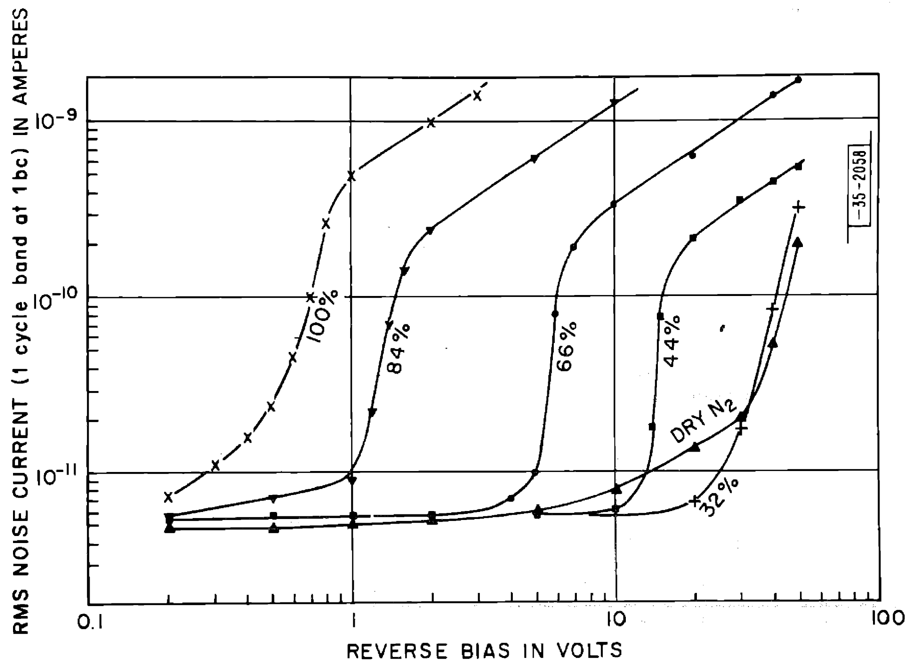

Fig. 5-4. Noise vs reverse bias at several values of relative humidity for the junction of Fig. 5-3. These measurements were made at the time that the third curve of Fig. 5-3 was taken.

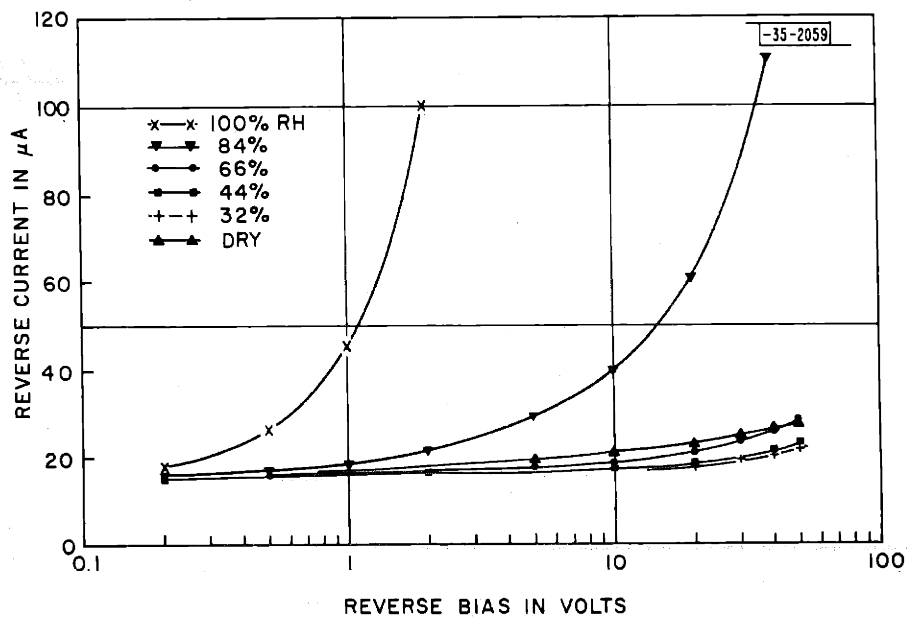

Fig. 5-5. Current-voltage characteristics corresponding to the curves of Fig. 5-4.

near 15 v at 44 per cent relative humidity, where the increase in noise is quite steep. In fact at this humidity and voltage the junction was unstable. When a bias of 15 volts was suddenly applied, the noise remained at a low level for a few seconds and then abruptly began to rise, taking about 30 seconds to increase some 20 db to a new steady value.

It should be emphasized that there was no change in the spectrum or in the broad-band appearance of the noise on an oscilloscope during these sudden increases in the noise level. The noise behaved just as if an attenuator were being cut out of the circuit. At 32 per cent relative humidity and at dry nitrogen, however, there were the usual popping effects and changes in spectrum at high voltages.

In addition to the special effects observed in the critical voltage region, the 1/f noise also shows the same transient behavior as the excess reverse currents. The noise associated with the leakage current tends to overshoot after an increase in the bias, while the noise associated with the channel normally builds up slowly. All of the data presented in this section were taken after the transient period was over.

<u>1/f Noise Associated with Leakage Current</u>

From Fig. 5-1 and 5-4 we have seen that the leakage current seems to produce a noise whose power increases approximately with the square of the dc voltage. It may also be shown from Fig. 5-4 and 5-5 that above the critical voltage the noise power at a fixed bias varies roughly as the first power of the conductance G of the leakage path. These two observations indicate that

$$\overline{\Delta i^2} = V^2 \, \overline{\Delta G^2} \propto V^2 \, \overline{G} \, , \qquad (5.1)$$

which in turn implies that $\overline{\Delta G^2} \propto \overline{G}$. This is just what would be expected if the leakage path is composed of a large number of parallel paths, with the

conductance of each fluctuating independently. However, to carry this idea further would require more knowledge about the physical origin of the leakage current.

1/f Noise Associated with Channel Current

The channel had originally been suspected of being the most important source of noise in p-n junctions. According to the Shockley-Montgomery theory for 1/f noise, the fluctuation in a germanium filament was produced by a noisy injection of hole-electron pairs from the surface. In a p-n junction only those minority carriers created within about a diffusion length of the junction are normally collected. But if a channel is present, all of the minority carriers generated in the channel area are collected as well. On the basis of the Shockley-Montgomery theory it had therefore been expected that the 1/f noise would increase in direct proportion to the channel length, just as the excess reverse current did. In connection with Fig. 5-3, it has been shown that such a voltage dependence is not obtained, while Fig. 5-1 and 5-4 indicate that in wet ambients the channel noise forms only a minor part of the total 1/f noise.

As a result of such observations, the theory for 1/f noise in germanium filaments was re-examined, which eventually led to the model proposed in Chapter III. That model will now be used to analyze two mechanisms which might be producing 1/f noise in channels: fluctuations in the surface generation rate, as discussed above, and fluctuations in the conductivity of the surface layer.

A. Fluctuations in Surface Generation Rate

From (4.6) we find that J_c, the current per unit area flowing across the surface junction of a channel, is given by

$$J_c = J_{cb} + J_{cs} = J_{cb} + \frac{q c_n c_p (n_i^2 - n_s p_s) N_t}{c_n(n_s + n_{s1}) + c_p(p_s + p_{s1})} , \qquad (5.2)$$

where J_{cb} and J_{cs} are, respectively, the bulk and surface components of J_c. In this section we wish to compute the noise produced by the fluctuations of J_c.

In Chapter III a variation in the net surface generation rate was obtained from a fluctuation in the product $n_s p_s$ in the numerator of the J_{cs} term. It was assumed that $|\phi_s| < |E_t - E_i|$, where E_t is here the energy level of the recombination centers, so that the "recombination coefficient"

$$r = \frac{c_n c_p N_t}{c_n(n_s + n_{s1}) + c_p(p_s + p_{s1})} \qquad (5.3)$$

could be taken as a constant.

In a channel it is impossible to achieve a fluctuation of J_c in this way because $n_s p_s$ is zero for all practical purposes. Every minority carrier generated in the channel is immediately swept into the bulk, thereby preventing any recombination from taking place. Under these circumstances J_c becomes

$$J_c = J_{cb} + \frac{q c_n c_p n_i^2 N_t}{c_n(n_s + n_{s1}) + c_p(p_s + p_{s1})} . \qquad (5.4)$$

Since the bulk generation J_{cb} would not be expected to show 1/f noise, any 1/f fluctuations in J_c must come from variations in n_s and p_s in the denominator of the expression for J_{cs}, or equivalently, from a variation in the recombination coefficient (5.3). This is apparently the type of noisy generation that was considered by Shockley. As can be seen from Fig. 4-6, the fluctuation in J_{cs} should be very small as long as the equilibrium value of ϕ_s is on the plateau of the generation curve, but might become appreciable on the slopes where $|\phi_s| > |E_t - E_i|$.

For the purpose of calculation we will assume a p-type channel on the n-side of the junction. Since n_s will then be nearly zero, the changes in J_c are produced by changes in p_s:

$$\delta J_c = -\frac{q N_t c_n c_p n_i^2}{\left[c_n n_{s1} + c_p(p_{so}+p_{s1})\right]^2} c_p \delta p_s \qquad (5.5)$$

$$= -\frac{J_{cs} c_p}{c_n n_{s1} + c_p(p_{so}+p_{s1})} \delta p_s .$$

As in the analysis of Chapter III, the surface area will be divided up into regions which are assumed small enough to contain a uniform trap structure, but large enough for δp_s to fluctuate independently in each one. The power spectrum for the fluctuations of δp_s may be obtained in essentially the same way, although there are a few changes due to the channel structure.

The integrated change in the surface concentration of holes which is produced by one additional electron in the traps is still given by (B.21) of Appendix B:

$$\delta \int p_s \, da = p_{so} \frac{q E_{so}}{kT} \frac{1}{\rho_{so}/q} , \qquad (5.6)$$

where the integration is over the surface. For p-type channels on the n-side, $\rho_{so}/q = N_D + p_{so}$. If the free hole charge is small compared with the charge produced by the donor impurities in the depletion layer, an approximate solution of Poisson's equation gives for the field at the surface

$$E_{so} = \left[2 q N_D (V + \phi_n + \phi_s)/\kappa\varepsilon_o\right]^{\frac{1}{2}} , \qquad (5.7)$$

where V, ϕ_n, and ϕ_s are defined for a p-type channel in a way analogous to that given by Fig. 4-5 for an n-type channel. Therefore, (5.6) can again be written in the form

$$\delta \int p_s \, da = \frac{p_{so}}{N_o + P_o} , \qquad (5.8)$$

where now

$$N_o + P_o = \frac{kT}{qE_{so}} \frac{1}{\rho_{so}/q} = \frac{kT}{q[2qN_D(V+\phi_n+\phi_s)/\kappa\varepsilon_0]^{1/2}} \frac{1}{N_D + p_{so}} \cdot \quad (5.9)$$

If the derivation in Appendix C is modified by setting $n_s = 0$, it will be found that the power spectrum for the fluctuations of the number of electrons in the traps of one of the elementary regions, whose area will now be denoted by $(\Delta x)^2$ instead of S, is given by

$$G_{n_t(\Delta x)^2}(\omega) = (\Delta x)^2 (N_o + P_o) \frac{4\tau_p}{1+(\omega\tau_p)^2} , \quad (5.10)$$

where τ_p, defined in (C.8), is

$$\tau_p = \frac{N_o + P_o}{p_{so} n_{to} c_p} \quad (5.11)$$

and $(N_o + P_o)$ is given in (5.9). Equation (5.10) is for a specific τ_p. If we assume the usual $1/\tau$ distribution between a lower limit τ_1 and an upper limit τ_2, the expected value of the spectrum of $n_t(\Delta x)^2$ for $\omega\tau_1 \ll 1 \ll \omega\tau_2$ will be

$$G_{n_t(\Delta x)^2}(\omega) = (\Delta x)^2 (N_o + P_o) \frac{1}{\ln(\tau_2/\tau_1)} \frac{1}{f} \cdot \quad (5.12)$$

Using (5.8) we find for the fluctuation of $p_s(\Delta x)^2$

$$G_{p_s(\Delta x)^2}(\omega) = \left(\frac{p_{so}}{N_o + P_o}\right)^2 (N_o + P_o) \frac{(\Delta x)^2}{\ln(\tau_2/\tau_1)} \frac{1}{f} , \quad (5.13)$$

while (5.5) gives for the spectrum of $J_c\ (\ x)^2$

$$G_{J_c(\Delta x)^2}(\omega) = \frac{J_{cs}^2\, c_p^2}{[c_n n_{s1} + c_p(p_{so} + p_{s1})]^2} \frac{p_{so}^2}{N_o + P_o} \frac{(\Delta x)^2}{\ln(\tau_2/\tau_1)} \frac{1}{f} \cdot \quad (5.14)$$

The noise from each area of the channel must now be added up. If ϕ_s is assumed constant over the channel length, as was done in Chapter IV for the derivation of the channel current, then J_{cs} and p_{so} are independent of the position of the elementary area. However, the quantity $(N_o + P_o)$ is not

since (5.9) shows that it is a function of V.

The summation of the regions around the circumference of the sample simply multiplies (5.14) by $C/\Delta x$, where C is the circumference. If the summation along the length of the channel is replaced by an integration, Equations (5.14) and (5.9) give for the spectrum of the total channel current

$$G_I(\omega) = \frac{1}{\ln(\tau_2/\tau_1)} \frac{C J_{cs}^2 c_p^2}{\left[c_n n_{s1} + c_p(p_{so}+p_{s1})\right]^2} \frac{p_{so}^2}{N_o+P_o} \frac{q}{kT}\left(\frac{2qN_D}{K\varepsilon_o}\right)^{\frac{1}{2}} \int_0^{\ell} \psi^{\frac{1}{2}}\, dx \quad \frac{1}{f}, \qquad (5.15)$$

where $\psi = V + \phi_n + \phi_s$. To perform this integration, we must know the functional dependence of ψ on x. The theoretical relation, obtained by integrating (4.3), is

$$\psi = \psi_o \exp\left[A J_c \left(x\ell - \frac{x^2}{2}\right)\right], \qquad (5.16)$$

where $\psi_o = V_o + \phi_n + \phi_s$. However, it has been seen that the experimental curves usually show a relation more like

$$\psi = \psi_o \exp\left(\frac{\ell - x}{a}\right), \qquad (5.17)$$

where a is some constant. If we use (5.17) rather than (5.16), then

$$G_I(\omega) = \frac{1}{\ln(\tau_2/\tau_1)} \frac{2CJ_c^2 c_p^2 a}{\left[c_n n_{s1} + c_p(p_{so}+p_{s1})\right]^2} \frac{p_{so}^2}{N_D + p_{so}} \frac{q}{kT}\left(\frac{2qN_D}{K\varepsilon_o}\right)^{\frac{1}{2}} \left(\psi_A^{\frac{1}{2}} - \psi_o^{\frac{1}{2}}\right) \frac{1}{f}, \qquad (5.18)$$

where $\psi_A = V_A + \phi_n + \phi_s$, and V_A is the applied voltage. The discussion of this formula will be postponed until after the derivation of the channel conductivity fluctuation.

B. Fluctuations in Channel Conductivity

The filling and emptying of the slow traps can produce a fluctuation in the number of majority carriers, and hence a fluctuation in the channel conductivity, in the same way as described for filaments in Chapter III. Since a change in the conductivity will cause the length of the channel to change slightly, these conductivity fluctuations will produce a fluctuation in the

total channel current. There is one complicating factor in the case of a channel, however, which is not encountered in a filament. When the conductivity of one region changes, the voltage distribution all along the channel must readjust since the applied voltage is fixed. This in turn alters the conductivity of every other region because the conductivity is a function of the voltage.

It will be assumed that the change in conductivity produced by the readjustment of the voltage follows the dc static characteristics. This is not completely true, but at the lower frequencies it should be a reasonable approximation. Because of the uncertainty over the correct expression for the channel conductivity as a function of the voltage, the conductivity will first be written simply as $\sigma(V)$. Then (4.3) becomes

$$\sigma(V)\frac{dV}{dx} = -J_c(\ell - x) \quad . \tag{5.19}$$

Denoting the equilibrium values by $\sigma_o(V_o)$ and V_o, and the deviation from equilibrium by $\delta\sigma$ and δV, we have

$$\left[\sigma_o(V_o) + \delta\sigma\right]\left[\frac{dV_o}{dx} + \frac{d}{dx}\delta V\right] = -J_c(\ell - x) - J_c\Delta\ell \quad . \tag{5.20}$$

To a linear approximation this gives

$$\sigma_o(V_o)\frac{dV_o}{dx} = -J_c(\ell - x) \tag{5.21a}$$

$$\delta\sigma\frac{dV_o}{dx} + \sigma_o(V_o)\frac{d}{dx}\delta(V) = -J_c\Delta\ell \quad . \tag{5.21b}$$

As before, the surface will be divided up into small regions of area $(\Delta x)^2$, and the noise produced by the fluctuation in the occupancy of the slow traps will be obtained separately for each region. These contributions will then be added up, assuming that the trap occupancy in each region fluctuates independently.

We will write $\delta\sigma$ as $\delta\sigma_1 + \delta\sigma_2$, where $\delta\sigma_1$ is the change in the conductivity produced by a change in the trap occupancy of the region under consideration, whose location will be taken at $x = x_o$, and where $\delta\sigma_2$ is the change in conductivity produced by the voltage readjustment. The assumption that the changes in σ follow the dc characteristics gives

$$\delta\sigma_2(x) = \left.\frac{d\sigma_o}{dV_o}\right|_{V=V_o(x)} \delta V(x) \ . \tag{5.22}$$

Hence (5.21b) becomes

$$\delta\sigma_1 \frac{dV_o}{dx} + \delta\sigma_2 \frac{dV_o}{dx} + \sigma_o(V_o)\frac{d\,\delta V}{dx} = \delta\sigma_1 \frac{dV_o}{dx} + \frac{d}{dx}(\sigma_o \delta V) = -J_c \Delta\ell \ . \tag{5.23}$$

Integrating from $x = 0$ to $x = \ell$, we obtain

$$\delta\sigma_1 \left.\frac{dV_o}{dx}\right|_{x=x_o} \Delta x + \sigma_o \delta V\Big|_{x=\ell} - \sigma_o \delta V\Big|_{x=0} = -\ell J_c \Delta\ell \ . \tag{5.24}$$

Since $\delta V = 0$ at $x = 0$ and $x = \ell$, we get

$$\Delta\ell = -\frac{\delta\sigma_1 \left.\frac{dV_o}{dx}\right|_{x=x_o} \Delta x}{\ell J_c} \ , \tag{5.25}$$

which becomes with the use of (5.21a)

$$\Delta\ell = \frac{\frac{\delta\sigma_1}{\sigma_o}(\ell - x_o)}{\ell} \Delta x \ . \tag{5.26}$$

Therefore, the change in current due to a change in conductivity $\delta\sigma_1$ in a region of area $(\Delta x)^2$, which is located at the point $x = x_o$, is

$$\Delta I = CJ_c\Delta\ell = \frac{\ell - x_o}{\ell} CJ_c \Delta x \frac{\delta\sigma_1}{\sigma_o} \ . \tag{5.27}$$

If we again assume a p-type channel on the n-side of the junction, the conductivity is[34]

$$\sigma_o = q\left(\frac{kT}{qE_{so}} P_{so}\right)\mu_{eff} \ , \tag{5.28}$$

where μ_{eff} is the effective channel mobility[43] and E_{so} is given by (5.7).

If the channel is not so strong that $p_{so} \gg N_D$, it may be shown that $\delta\mu_{eff}/\mu_{eff}$ is negligible in comparison with $\delta p_s/p_{so}$ for a small change in ϕ_s. Under these conditions

$$\frac{\delta\sigma_1}{\sigma_0} = \frac{\Delta x}{C} \frac{\delta p_s}{p_{so}} . \tag{5.29}$$

Hence (5.27) becomes

$$\Delta I = \frac{\ell - x_0}{\ell} (C J_c \Delta x) \frac{\Delta x}{C} \frac{\delta p_s}{p_{so}} . \tag{5.30}$$

In (5.13) we had for the power spectrum for the fluctuations of $p_s(\Delta x)^2$

$$G_{p_s(\Delta x)^2}(\omega) = \frac{p_{so}^2}{N_0 + P_0} \frac{(\Delta x)^2}{\ln(\tau_2/\tau_1)} \frac{1}{f} . \tag{5.31}$$

Therefore, the current noise due to the one region under consideration is

$$G_{I_{(\Delta x)^2}}(\omega) = \left(\frac{\ell - x_0}{\ell}\right)^2 \frac{J_c^2}{N_0 + P_0} \frac{(\Delta x)^2}{\ln(\tau_2/\tau_1)} \frac{1}{f} . \tag{5.32}$$

We must now sum up the noise produced by each of the elementary regions of area $(\Delta x)^2$. The problem is essentially the same as that met in connection with (5.14) for the fluctuation in the generation rate. However, in (5.32) the factor $(\ell - x_0)^2$ varies with the position of $(\Delta x)^2$ as well as $(N_0 + P_0)$. If we again use (5.17) for the functional dependence between V and x, integration of (5.32) over the channel surface gives for the total current noise

$$G_I(\omega) = \frac{1}{\ln(\tau_2/\tau_1)} \frac{2CJ_c^2 a}{N_D + p_{so}} \frac{q}{kT} \left(\frac{2qN_D}{K\epsilon_0}\right)^{\frac{1}{2}} \left[\left(1 - \frac{4a}{\ell} - \frac{8a^2}{\ell^2}\right)\psi_A^{\frac{1}{2}} - \frac{8a^2}{\ell^2}\psi_0^{\frac{1}{2}}\right| \frac{1}{f} . \tag{5.33}$$

C. <u>Discussion of Channel Noise</u>

For biases greater than about a volt, the two noise expressions derived in the preceding sections become approximately:

1) Fluctuations in surface generation

$$N_{gen}(\omega) = \frac{1}{\ln(\tau_2/\tau_1)} \frac{2CJ_{cs}^2 a}{N_D + p_{so}} \left[\frac{c_p p_{so}}{c_n n_{s1} + c_p(p_{so}+p_{s1})} \right]^2 \frac{q}{kT} \left(\frac{2qN_D}{K\varepsilon_0} \right)^{\frac{1}{2}} V_A^{\frac{1}{2}} \frac{1}{f} \tag{5.34}$$

2) Fluctuations in channel conductivity

$$N_{cond}(\omega) = \frac{1}{\ln(\tau_2/\tau_1)} \frac{2CJ_{cs}^2 a}{N_D + p_{so}} \frac{q}{kT} \left(\frac{2qN_D}{K\varepsilon_0} \right)^{\frac{1}{2}} V_A^{\frac{1}{2}} \frac{1}{f} \tag{5.35}$$

As previously mentioned, neither formula gives the right voltage dependence. Both predict that the noise power should increase approximately as $V^{1/2}$, while the experimental curves of Fig. 5-3 give a voltage dependence which is more nearly proportional to the first power of V. However, we will show that the fluctuation in channel conductivity gives about the right order of magnitude for the noise, while the fluctuation in generation rate gives a much smaller value. The ratio of the two noise expressions is

$$\frac{N_{cond}}{N_{gen}} = \left(\frac{J_c}{J_{cs}} \right)^2 \left[\frac{c_n n_{s1} + c_p(p_{so}+p_{s1})}{c_p p_{so}} \right]^2 . \tag{5.36}$$

When $|\phi_s| < |E_t - E_i|$, the factor $[c_n n_{s1} + c_p (p_{so} + p_{s1})]^2/p_{so}^2$ is much greater than unity. On the other hand, if $|\phi_s| > |E_t - E_i|$, the factor $(J_c/J_{cs})^2$ becomes very large, since J_c approaches a constant value J_{cb} while J_{cs} approaches zero. Hence in both cases N_{cond} is greater than N_{gen}. If for $|\phi_s| < |E_t - E_i|$, we assume $J_c \sim J_{cs}$, $c_n \sim c_p$, and $|E_t - E_i| = 0.20$ ev, the ratio (5.36) is about 3000 for $\phi_s = 0.10$ ev.

In order to make the order-of-magnitude calculation for (5.35), we need approximate values for C, J_c, a, p_{so}, and N_D. The quantity a was defined by (5.17):

$$(V + \phi_n + \phi_s) = (V_0 + \phi_n + \phi_s) \exp\left(\frac{\ell - x}{a} \right) .$$

Therefore, the total channel current I_c would be

$$I_c = C J_c \ell = C J_c a \ln \frac{V_A + \phi_n + \phi_s}{V_o + \phi_n + \phi_s} . \qquad (5.37)$$

Although the curves of Fig. 5-2 do not accurately follow (5.37), it is possible to obtain a rough value of $CJ_c a = 7\ \mu A$ for the middle curve. For the other parameters we have $J_c \simeq 500\ \mu A/cm^2$ (the bulk generation is larger here than for channels on the p-side encountered in Chapter IV), $N_D = 2 \times 10^{14}/cm^3$ for the 9 ohm-cm n-type material, and $p_{so} \sim N_D$. Taking $\tau_2/\tau_1 \sim 10^8$, as was done in Chapter III, we find that the noise power at a bias of 10 v and a frequency of 1 kc is approximately

$$N_{cond}(\omega) \simeq \frac{1}{20} \frac{2(7\times 10^{-6})(500\times 10^{-6})}{2(2\times 10^{14})} \frac{1}{.026} \left(\frac{2\times 1.6\times 10^{-19} \times 2\times 10^{14}}{16\times 88\times 10^{-14}} \right)^{\frac{1}{2}} 10^{\frac{1}{2}} \frac{1}{1000}$$
$$\simeq 7\times 10^{22}\ amp^2/cycle . \qquad (5.38)$$

Hence the rms current in a one cycle band at V = 10 v and f = 1 kc is about 2.5×10^{-11} amp. This value is in reasonable agreement with the noise curves of Fig. 5-3.

Since the voltage dependence, and also the relative magnitude, of the three curves of Fig. 5-3 are given incorrectly by (5.35), an attempt was made to fit the experimental curves with an empirical formula. It was found that by simply multiplying (5.35) by I_c^2, the square of the total channel current, good agreement could be obtained with Fig. 5-3. The resulting formula is

$$N_{cond} = const. \frac{a}{N_D + p_{so}} I_c^2 V_A^{\frac{1}{2}} \frac{1}{f} . \qquad (5.39)$$

Since p_{so} is not known exactly, the values of (5.39) were computed with the factor $1/(p_{so} + N_D)$ omitted. The relative values of the parameter a were determined from Fig. 5-2, while the one arbitrary constant in (5.39) was adjusted for the best fit with the second curve of Fig. 5-3. Except for

the high voltage regions of the second and third curves, where the popping noise was encountered, the agreement in shape is quite good. The values predicted by (5.39) without the factor $1/(p_{so} + N_D)$ are somewhat high for the first curve. If this factor were included, it would tend to make the agreement even better.

This result, coupled with the previous order-of-magnitude calculation, are perhaps as much as can be expected until the dc characteristics of the channel are more completely understood.

CHAPTER VI

EXTENSIONS OF 1/f NOISE MODEL

Most of the sources of 1/f noise involve current passing through or over potential barriers. This class includes carbon resistors and microphones, granular metallic films, point-contact diodes and transistors, some photoconductors, and the cathode interface resistance in vacuum tubes. To explain the 1/f noise in these devices, it seems most promising to look for some mechanism which can produce changes in the height of the potential barrier. Many investigators have turned to processes involving adsorption and desorption of ions or diffusion of ions in order to get the very long time constants found at room temperature in 1/f noise. But the discussion in Chapter I showed that such ionic mechanisms cannot give the short time constants observed at low temperatures.

It is possible, however, to get long time constants from the purely electronic process of trapping. Furthermore, if traps were located in or adjacent to the potential barrier, the fluctuation in localized charge resulting from the filling and emptying of the traps could give the desired fluctuation in the height of the barrier. Assuming the traps act independently, each one by itself would only give shot noise. Therefore, it would be necessary to have a distribution of traps with different time constants in order to obtain a 1/f spectrum. In Appendix A it has been shown that a distribution of the traps in energy will not work. However, if we assume that the traps are located in the potential barrier and communicate with the bulk by electrons tunneling through the barrier, a 1/f spectrum can be

obtained in a completely natural manner. A small variation in the barrier height or width for tunneling can easily give the required range of time constants without an accompanying temperature dependence. Since such a variation would change the effective capture cross-section for the traps, and hence the expected lifetime of both the filled and the empty state, a $1/\tau$ distribution for the time constants is needed to obtain a 1/f spectrum (see Appendix A). But as has been shown in Chapter III, the tunneling process will give a $1/\tau$ distribution if the traps are simply distributed homogeneously throughout the barrier region.

In order to explore these ideas somewhat further, and also to get away from bulk semiconductor properties, a contact between a mercury drop and a piece of aluminum was examined for possible 1/f noise. Since mercury does not wet aluminum oxide, it was expected that the thin oxide layer on aluminum would form a potential barrier between the two metals. Hence, traps in the oxide might produce 1/f fluctuations in the manner just described. The reason for using mercury as the other electrode was primarily to avoid any mechanical disturbance of the oxide, but mercury also has the advantage of simplicity. As will be shown in the next section, the experiment was quite successful in that the oxide layer does act like a potential barrier, and a strong 1/f noise with all of the usual characteristics is produced by the contact. However, the work has not been carried far enough to decide definitely whether the trapping model is correct.

<u>Experimental Results</u>

A low resistance, noiseless contact was made to one side of a small square of aluminum with an ultrasonic soldering iron, while the other side was cleaned and polished. The aluminum was then oxidized at 100° C for

several hours, which resulted in an oxide layer probably 30 to 40 Å thick. The mercury drop, usually around 0.01 cm^2 in area, was placed on the polished side, and a noiseless contact made to the mercury with a clean platinum wire.

The dc current-voltage characteristics of several contacts formed in this manner were linear from about -0.2 to +0.2 volts, with the resistance usually between 10 K and 100 K. Because of the extremely large fields produced across the thin oxide layer, higher voltages resulted in breakdown. This was especially pronounced when the aluminum was the cathode, for then the mercury would bridge across the oxide layer and short out the contact.

It had been anticipated that electrons would pass through the oxide by tunneling rather than by thermionic excitation over the barrier, in which case the resistance would not appreciably change with temperature. This is precisely what was observed from room temperature down to liquid nitrogen temperature, the freezing of the mercury having no apparent effect. Typical current-voltage characteristics for the two-temperature extremes are shown in Fig. 6-1.

As Fig. 6-2 illustrates for the same sample, the ac characteristics of these contacts were those of a simple parallel RC network. Since the frequency response curves must be used to correct the noise data, the 100K generator impedance employed in the noise measurements was left across the sample during the ac measurements. Taking this fact into consideration and using the resistance indicated by Fig. 6-1, we find that the capacitance must be of the order of 0.01 μf. This value agrees with the theoretical capacitance calculated from the geometry

$$C = \frac{\kappa \varepsilon_0 A}{d} = \frac{5 \times 8.8 \times 10^{-14} (.01)}{40 \times 10^{-8}} \simeq 0.01 \times 10^{-6} f ,$$

where we have taken $\kappa \simeq 5$.

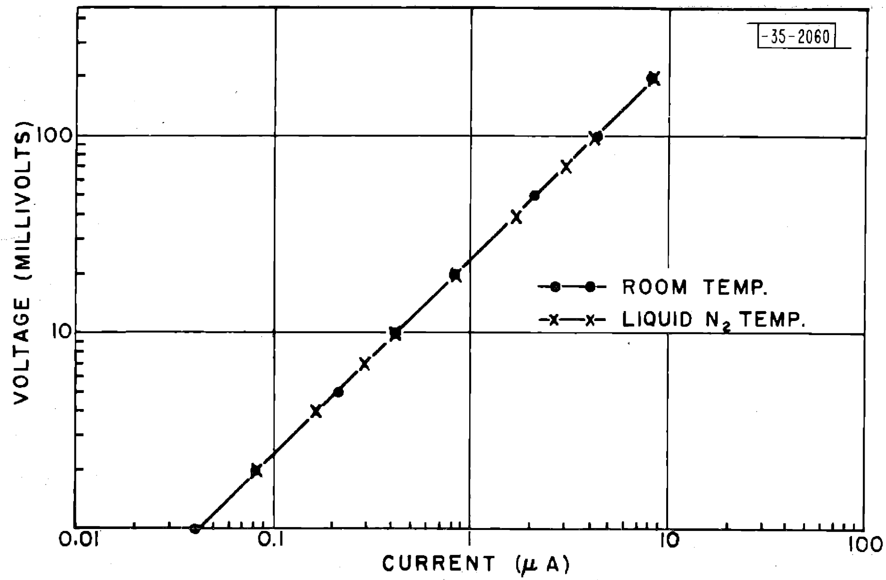

Fig. 6-1 DC current-voltage characteristics of a mercury-aluminum contact at room and liquid nitrogen temperature.

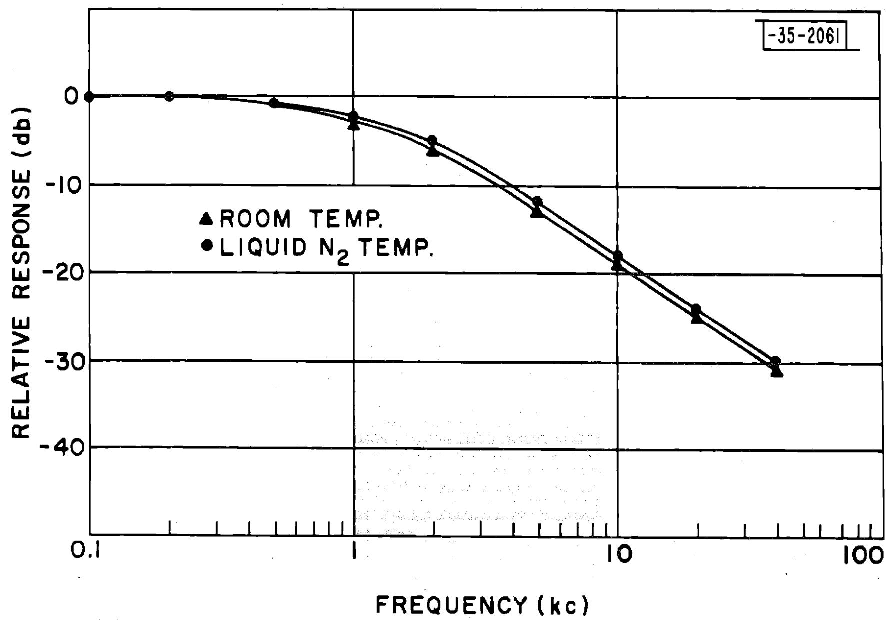

Fig. 6-2. Relative frequency response at room and liquid nitrogen temperature for the contact of Fig. 6-1.

As was hoped, the contact showed a very large voltage fluctuation when dc current was applied. The noise power obeyed quite accurately a 1/f law over the measured range of frequencies, 100 cps to 40 kc, and increased with the square of the dc current in the characteristic way for 1/f noise. Figure 6-3 shows the amplitude of the noise at 1 kc as a function of the dc current for two different contacts. The two curves at room temperature for Sample A, which is the one that has been used to illustrate the dc characteristics, were taken before and after the run at liquid nitrogen temperature. For Sample A at the lower currents the noise decreased only about 2 db in going down to liquid nitrogen temperature. On other contacts the drop was occasionally as much as 6 or 8 db, while in some cases the amplitude appeared to remain almost constant. At liquid nitrogen temperature the noise level for a few contacts, including Sample A, was unstable for biases greater than 50 mV and showed a marked deviation from the I^2 dependence. However, neither the current-voltage curves nor the spectrum measurements indicated anything unusual in this region.

Examples of the frequency dependence of the noise are given in Fig. 6-4 for two extremes, high voltage at liquid nitrogen temperature, and low voltage at room temperature. The solid curves show the actual data points, which must be corrected for the ac response of the RC circuit in order to get the true spectrum of the resistance fluctuations. When this is done with the aid of Fig. 6-2, we obtain in both cases a set of points which can be fitted by a $1/f^{1.0}$ law within experimental accuracy. The internal noise of the amplifier was about 50 db below 1 μv at the higher frequencies, so only a partial spectrum could be obtained at low bias currents. As would be expected from the linearity of the dc characteristics, the polarity of the bias current had no effect on the noise.

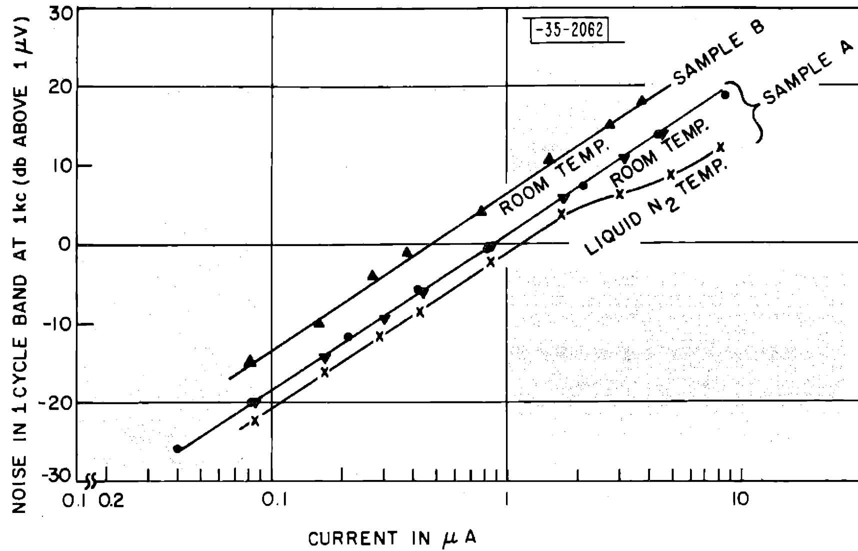

Fig. 6-3. Dependence of noise power on dc current for two samples.

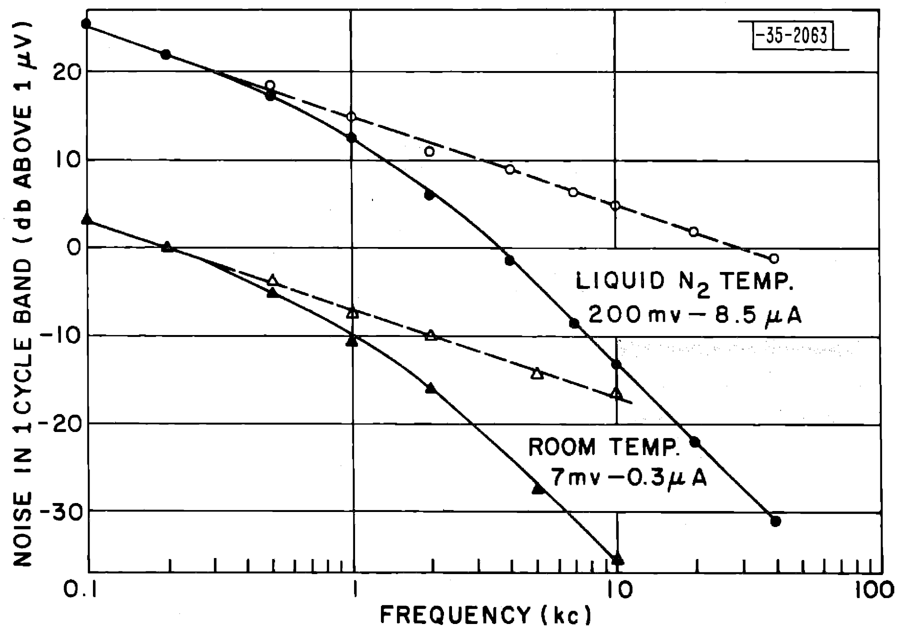

Fig. 6-4. Power spectrum for noise at two extremes of dc bias and temperature. The solid lines correspond to the actual data points, while the dashed lines show the spectrum after correction for the frequency response of the contact.

Discussion

As far as the dc and average ac characteristics of the mercury-aluminum contact are concerned, the aluminum oxide seems to form a simple potential barrier between two metals, through which electrons can pass by tunneling. No semiconductor properties of the oxide appear to be involved since the resistivity does not change with temperature. Calculations of the dc resistance to be expected from the tunneling process, which were carried out using formulas given by Holm,[51] show that agreement can be obtained with the experimental values by assuming a barrier with a height of about 1 ev and a width of 30 to 40 Å. These observations, incidentally, give strong support to Mott's hypothesis that in the oxidation of aluminum, the adsorbed oxygen is easily ionized by electrons tunneling through the oxide.[52] Cabrera[53] has also found that the influence of ultraviolet light on the oxidation of aluminum can be explained by assuming the same model.

Traps in the oxide layer could arise physically from impurities, a deviation from stoichiometry, or other crystalline imperfections. If we postulate the existence of traps, and a few will almost certainly be present, it is quite plausible in view of the dc characteristics of the contact to assume that they communicate with the metals by tunneling. As previously discussed, a 1/f spectrum for the conductivity fluctuations will then be obtained if the traps are homogeneously distributed throughout the oxide layer.

In addition to the shape of the spectrum, the model should also account for the magnitude of the noise, the value of the dc resistance, and the range of the time constants. If the height and width of the potential barrier formed by the oxide were completely uniform over the area of the contact,

it would not be possible to get both the observed value of the dc resistance and the long time constants for the traps. However, a preliminary analysis based only on general conductivity fluctuations has indicated that in order to get the magnitude of the 1/f noise, it is necessary to assume that the current is carried by an extremely small fraction of the total area of the contact. This would suggest that there are a few places where the oxide layer is thin or the barrier somewhat low, and that these spots carry practically all of the current. Traps located in normal regions just outside of the "weak" spots could then strongly modulate the conductivity, but still have time constants as long as are needed for 1/f noise. To carry this model much further, it would be desirable to have some independent proof of the existence of traps in aluminum oxide and the $1/\tau$ distribution of time constants; or in other words, information similar to that supplied by the field effect experiment about germanium.

APPENDIX A

We will consider a general class of models for 1/f noise in which the slow emptying and filling of traps is used to modulate the conductivity, and where it is assumed that each trap acts independently of the others. It will first be shown that a uniform distribution of energy levels for the traps will not lead to a 1/f spectrum. For simplicity, the argument will be confined to traps which communicate with only one band, which will be taken as the conduction band for the sake of discussion. This is not really an important restriction, since any bulk trap which can give the long times needed for 1/f noise would almost have to satisfy such a condition.

Let $1/\sigma$ be the probability per unit time that the trap emits an electron to the conduction band, given that the trap is full; and let $1/\tau$ be the probability per unit time that the trap captures an electron from the conduction band, given that the trap is empty. Hence σ is the expected lifetime of the filled state, and τ is the expected lifetime of the empty state. The time τ is given by

$$\tau = 1/S v N_c \exp\left[-(E_c - E_F)/kT\right] , \qquad (A.1)$$

where S is the capture cross-section of the trap and v is the thermal velocity of the free electrons. Since $\sigma/(\sigma+\tau)$ is the average time that the trap is full, we have from Fermi-Dirac statistics that

$$\sigma/(\sigma+\tau) = 1/\left[1 + \exp(E_t - E_F)/kT\right] , \qquad (A.2)$$

where E_t is the effective energy level of the trap. Therefore,

$$\sigma = 1/S v N_c \exp\left[-(E_c - E_t)/kT\right] . \qquad (A.3)$$

This relation for σ could also have been obtained from a detailed balancing argument.

The filling and emptying of the trap forms a two-state Markov process, for which the power spectrum is (see, for example, reference 54)

$$G(\omega) = \frac{1}{\sigma + \tau} \frac{4T^2}{1 + (\omega T)^2} , \tag{A.4}$$

where

$$\frac{1}{T} = \frac{1}{\sigma} + \frac{1}{\tau} . \tag{A.5}$$

$G(\omega)$ is defined here on a per cycle basis for positive frequencies only.

For the trap levels which are above the Fermi level, we have $\sigma < \tau$. The power spectrum for these traps then becomes approximately

$$G(\omega) \simeq \frac{1}{\tau} \frac{4\sigma^2}{1 + (\omega\sigma^2)} . \tag{A.6}$$

Now suppose one tries to obtain a 1/f spectrum by superimposing such spectra with a distribution for the energy levels of the traps. If the capture cross-section S is assumed to remain approximately constant as the trap depth varies, as will normally be the case, τ will be independent of the energy level E_t, while σ will vary exponentially with E_t. It is easily verified that the weighting factor needed to get a 1/f spectrum from (A.6) is $1/\sigma^2$, whereas a uniform distribution of energy levels corresponds to a $1/\sigma$ weighting factor On the other hand, for the traps below the Fermi level, τ is smaller than σ, and (A.4) takes the form

$$G(\omega) \simeq \frac{1}{\sigma} \frac{4\tau^2}{1 + (\omega\tau)^2} . \tag{A.7}$$

Since τ will still be practically independent of the trap depth, a distribution of energy levels cannot give a 1/f spectrum under these circumstances. Only σ will change, and this merely alters the constant in front of the shot noise spectrum, $\tau^2/[1 + (\omega\tau)^2]$.

Therefore, only the traps above the Fermi level can be used to obtain a 1/f spectrum from a distribution in energy levels, and in this case the

energy distribution must correspond to a distribution for σ which is proportional to $1/\sigma^2$. However, we will next show that the latter requirement cannot be met over a range of temperature. If $N(E_t)$ is the number of trap levels per unit energy, we must have for a $1/\sigma^2$ weighting factor

$$N(E_t) \propto \frac{1}{\sigma^2(E_t)}\frac{d\sigma}{dE_t} = \frac{1}{\sigma^2}\frac{\sigma}{kT} \propto \frac{exp[-(E_c - E_t)/kT]}{kT} . \tag{A.8}$$

Suppose we assume a distribution of energy levels which satisfies (A.8) at a temperature T_o; i.e., assume

$$N(E_t) \propto \frac{exp[-(E_c - E_t)/kT_o]}{kT_o} . \tag{A.9}$$

Then at a temperature $T_o/2$, the distribution function for σ, denoted by $W(\sigma)$, becomes

$$W(\sigma) \propto N(E_t)\frac{dE_t}{d\sigma} \propto \frac{1}{kT_o} exp[-(E_c - E_t)/kT_o]\frac{kT_o/2}{\sigma} \tag{A.10}$$

$$\propto \frac{1}{2}\sigma^{-\frac{1}{2}}\frac{1}{\sigma} = \frac{1}{2}\frac{1}{\sigma^{3/2}} ,$$

since at $T = T_o/2$

$$\sigma \propto exp\left[2(E_c - E_t)/kT_o\right] . \tag{A.11}$$

Thus even if one assumes the very special distribution of energy levels necessary to get a 1/f spectrum at room temperature, a different spectrum would be obtained at say liquid nitrogen temperature. Since the spectrum of 1/f noise seems to remain the same over this temperature range (and even down to liquid helium temperature in those cases where it has been measured), and since there is no experimental evidence for any exponential distribution of trap levels, it would appear that this method for obtaining a 1/f spectrum can be eliminated.

For germanium there is another interesting objection which may be raised. Just to get the experimental range of 8 decades of 1/f noise at

room temperature, it would be necessary to have a range of energy levels for the traps (above the Fermi level) of about $\frac{kT}{q} \ell n\, 10^8 \simeq 0.5$ ev. In high resistivity germanium there is not that much difference in energy between the Fermi level and either band. Furthermore, with normal capture cross-sections of the order of 10^{-14} cm^2, the range in energies would have to be between 0.5 and 1.0 ev in order to get time constants between 10^{-4} and 10^4 sec. Since the energy gap in germanium is only about 0.7 ev, the required range of energy levels cannot be obtained unless one assumes the existence of extremely high potentials barriers surrounding each trap. Such a condition seems impossible in the single-crystal germanium presently used.

In Chapter VI a model for 1/f noise will be proposed which leads to a wide range of effective capture cross-sections for traps. Since (A.2) and (A.3) show that both σ and τ are inversely proportional to S, we may write $\sigma = \alpha\tau$ for this type of variation. Then (A.4) becomes

$$G(\omega) = \frac{1}{(\alpha+1)\tau} \frac{4\left(\frac{\alpha\tau}{1+\alpha}\right)^2}{1+\left(\frac{\omega\alpha\tau}{1+\alpha}\right)^2} = \frac{\alpha}{(\alpha+1)^2} \frac{4\,\frac{\alpha\tau}{1+\alpha}}{1+\left(\frac{\omega\alpha\tau}{1+\alpha}\right)^2} . \qquad \text{(A.12)}$$

Hence in this case a $1/\tau$ distribution is needed for a 1/f spectrum.

APPENDIX B

<u>Derivation of N_o and P_o</u>

In (2.4) the quantities N_o and P_o were defined by

$$N_o = n_{so}\,\delta N/\delta n_s$$
$$P_o = p_{so}\,\delta P/p_{so}\ . \qquad \text{(B.1)}$$

If we denote the bulk equilibrium values of n and p by n_o and p_o, respectively, and assume that the surface under consideration is at x = 0, while the other surface is at x = $-\infty$, then δN and δP are the changes in

$$N = \int_{-\infty}^{0} (n - n_o)\,dx$$

and

$$P = \int_{-\infty}^{0} (p - p_o)\,dx\ , \qquad \text{(B.2)}$$

respectively. Using ϕ for the potential, Equations (B.2) may be rewritten as

$$N = \int_{-\infty}^{0} (n - n_o)\frac{dx}{d\phi}\,d\phi = -\int_{0}^{\phi_s}\frac{n - n_o}{E_x}\,d\phi$$
$$P = \int_{-\infty}^{0} (p - p_o)\frac{dx}{d\phi}\,d\phi = \int_{0}^{\phi_s}\frac{p - p_o}{E_x}\,d\phi\ , \qquad \text{(B.3)}$$

where E = $-d\phi/dx$ is the electric field. Hence to a linear approximation

$$N_o = n_{so}\frac{dN}{dn_s} = n_{so}\frac{dN}{d\phi_s}\frac{d\phi_s}{dn_s} = -n_{so}\left(\frac{n_{so} - n_o}{E_{so}}\right)\frac{kT}{q n_{so}} = -\frac{kT}{qE_{so}}(n_{so} - n_o)\ ,$$

and similarly (B.4)

$$P_o = p_{so}\frac{dP}{dp_s} = p_{so}\frac{dP}{d\phi_s}\frac{d\phi_s}{dp_s} = \frac{kT}{qE_{so}}(p_{so} - p_o)\ ,$$

where E_{so} is the equilibrium field at the surface.

To obtain E_{so} we must solve Poisson's equation

$$\frac{d^2\phi}{dx^2} = -\frac{\rho}{K\epsilon_o} = -\frac{q}{K\epsilon_o}\left(N_D - N_A + p - n\right)\ , \qquad \text{(B.5}$$

where N_D and N_A are the donor and acceptor densities, respectively. The requirement of charge neutrality deep within the bulk gives $N_D - N_A = n_o - p_o$. Writing the free carrier densities in the form

$$n = n_i \exp(q\phi/kT)$$
$$p = n_i \exp(-q\phi/kT) \ , \tag{B.6}$$

we have

$$\frac{d^2\phi}{dx^2} = -\frac{2qn_i}{K\varepsilon_o}\left(\sinh\frac{q\phi_B}{kT} - \sinh\frac{q\phi}{kT}\right) \ , \tag{B.7}$$

where ϕ_B is the bulk value of ϕ (see Fig. 1-1). Integration of (B.7) gives for the field at the surface

$$\frac{q}{kT}E_{so} = \pm\left(\frac{2q^2n_i}{K\varepsilon_o kT}\right)^{\frac{1}{2}}\left[2\left(\sinh\frac{q\phi_B}{kT}\right)\frac{q}{kT}(\phi_B - \phi_s) - 2\left(\cosh\frac{q\phi_B}{kT} - \cosh\frac{q\phi_s}{kT}\right)\right]^{\frac{1}{2}} . \tag{B.8}$$

Using (B.8) we find that the limiting form of (B.4) when $\phi_B = \phi_S$ is

$$N_o = n_o\left[\frac{K\varepsilon_o kT}{q^2(n_o+p_o)}\right]^{\frac{1}{2}}$$
$$P_o = p_o\left[\frac{K\varepsilon_o kT}{q^2(n_o+p_o)}\right]^{\frac{1}{2}} . \tag{B.9}$$

For nearly intrinsic germanium ($\phi_B \simeq 0$), an n-type surface gives

$$N_o \simeq n_{so}\left[\frac{K\varepsilon_o kT}{2q^2(n_{so}+p_{so})}\right]^{\frac{1}{2}}$$
$$P_o \ll N_o \ , \tag{B.10a}$$

while a p-type surface gives

$$P_o \simeq p_{so}\left[\frac{K\varepsilon_o kT}{2q^2(n_{so}+p_{so})}\right]^{\frac{1}{2}}$$
$$N_o \ll P_o \ . \tag{B.10b}$$

Equations (B.10a) and (B.10b) may be written together as

$$N_o + P_o \simeq (n_{so}+p_{so})\left[\frac{K\varepsilon_o kT}{2q^2(n_{so}+p_{so})}\right]^{\frac{1}{2}} . \tag{B.11}$$

Changes in Carrier Concentrations Produced by Trapping

We first wish to calculate the integrated change in the surface concentrations of holes and electrons which is produced by one additional electron in the traps. For this purpose we may set up a rectangular coordinate system with the origin at the surface of the germanium just beneath the trapped charge (the charge itself may be on the surface of the oxide, perhaps 30 Å from the germanium). Let the germanium surface be in the y-z plane, and let the positive direction of x be outward. To a linear approximation, the integrated change in the free carrier concentrations at the surface may be expressed in terms of the deviation from equilibrium of the surface potential ϕ_s:

$$\delta \int n_s \, dy\, dz = \int \frac{\partial n_s}{\partial \phi_s} \delta\phi_s \, dy\, dz = \frac{q}{kT} n_{so} \int \delta\phi_s \, dy\, dz \quad ,$$
$$\delta \int p_s \, dy\, dz = -\frac{q}{kT} p_{so} \int \delta\phi_s \, dy\, dz \, . \qquad \text{(B.12)}$$

To obtain the integrated value of $\delta\phi_s$, we must perform some manipulations on Poisson's equation,

$$\frac{\partial^2\phi}{\partial x^2} + \frac{\partial^2\phi}{\partial y^2} + \frac{\partial^2\phi}{\partial z^2} = -\frac{\rho}{K\varepsilon_0} \; . \qquad \text{(B.13)}$$

The deviation in potential due to the trapped electron and the charge it induces in the germanium will decay essentially to zero within a few Debye lengths of the origin.[42] It will be assumed that before the electron was trapped there was no variation of ϕ in the y-z plane, or at least a variation which is negligible over a distance of a Debye length, so that the terms $d^2\phi/dy^2$ and $d^2\phi/dz^2$ arise only from the trapped and induced charge. Hence, if we integrate (B.13) over an area A which is several Debye lengths square, the terms resulting from $d^2\phi/dy^2$ and $d^2\phi/dz^2$ will vanish, which may be proved by transforming these terms by Green's theorem into the integral of the

normal derivation around the periphery of A. Therefore, the integration over A gives

$$\frac{d^2f}{dx^2} = -\frac{1}{K\varepsilon_o}\int_A \rho\, dy\, dz \,, \tag{B.14}$$

where

$$f(x) = \int_A \phi(x,y,z)\, dy\, dz \,. \tag{B.15}$$

The integrated field normal to the surface is given by

$$F(x) = \int_A E_x\, dy\, dz = -\frac{df}{dx} \,. \tag{B.16}$$

Using this definition, Equation (B.15) may be rewritten as

$$F\frac{dF}{df} = -\frac{1}{K\varepsilon_o}\int_A \rho\, dy\, dz \,. \tag{B.17}$$

Hence a small deviation of f from equilibrium at the surface is given by

$$\delta f_s \simeq \frac{df}{dF}\,\delta F_s = -\frac{K\varepsilon_o F_{so}}{\int_A \rho_{so}\, dy\, dz}\,\delta F_s = -K\varepsilon_o \frac{A E_{so}}{A \rho_{so}}\,\delta F_s \,, \tag{B.18}$$

where F_{so}, E_{so} and ρ_{so} are the equilibrium values at the surface. But for one negative charge trapped

$$\delta F_s = \int_A \delta E_x\, dy\, dz = \frac{q}{K\varepsilon_o} \,. \tag{B.19}$$

Using (B.18) and (B.19) we find that

$$\begin{aligned}\delta\int n_s\, dy\, dz &= \frac{q}{kT} n_{so}\int \delta\phi_s\, dy\, dz = \frac{q}{kT} n_{so}\,\delta f_s \\ &= -\frac{q}{kT} n_{so} K\varepsilon_o \frac{E_{so}}{\rho_{so}}\,\delta F_s = -n_{so}\frac{qE_{so}}{kT}\frac{1}{\rho_{so}/q} \,.\end{aligned} \tag{B.20}$$

Since $\rho_{so}/q = p_{so} - n_{so} + N_D - N_A = (p_{so} - p_o) + (n_o - n_{so})$, we have, with the aid of (B.4),

$$\delta\int n_s\, dy\, dz = -\frac{n_{so}}{N_o + P_o} \,. \tag{B.21a}$$

Similarly,

$$\delta\int p_s\, dy\, dz = p_{so}\frac{qE_{so}}{kT}\frac{1}{\rho_{so}/q} = \frac{p_{so}}{N_o + P_o} \,. \tag{B.21b}$$

We will also need the corresponding relations for the change in the total number of free holes and electrons in the germanium produced by the trapped electron. Generalizing (B.2) and (B.3), we have for the change in the number of electrons

$$\int \delta N dydz = \delta \int_A dydz \int_{-\infty}^{0} (n-n_o)dx = -\delta \int_A dydz \int_0^{\phi_s(y,z)} \frac{n-n_o}{E_x} d\phi \ . \qquad (B.22)$$

Hence, with the usual linear approximation,

$$\begin{aligned} \int_A \delta N dydz &= \int_A \left[\frac{\partial}{\partial \phi_s} \int_0^{\phi_s(y,z)} \frac{n-n_o}{E_x} d\phi \right] \delta\phi_s(y,z) dydz \\ &= \int_A \frac{n_{so}-n_o}{E_{so}} \delta\phi_s(y,z) dydz = -\frac{n_{so}-n_o}{E_{so}} \delta f_s \qquad (B.23) \\ &= \frac{n_{so}-n_o}{E_{so}} \frac{K\epsilon_o E_{so}}{\rho_{so}} \frac{q}{K\epsilon_o} \ , \end{aligned}$$

where (B.18) and (B.19) have been used to evaluate δf_s. From (B.4) we then get

$$\int_A \delta N \, dydz = -\frac{N_o}{N_o + P_o} \ . \qquad (B.24a)$$

The relation for the change in the number of free holes, which can be obtained in a similar manner, is

$$\int_A \delta P dydz = \frac{P_o}{N_o + P_o} \ . \qquad (B.24b)$$

APPENDIX C

The fluctuation in the number of electrons in the traps forms a "birth and death" type of process, for which there exist standard techniques of analysis.[55] The first step will be to obtain a set of differential equations for the probability of a specified number of electrons being in the traps at a time t. This essentially involves setting up (2.2) again, but this time on a probability basis.

If we denote the area of the elementary regions by S, then the probability that there are $(Sn_{to} + k)$ electrons in the traps at time $(t + \Delta t)$ is given by the sum of the probabilities of the following six mutually exclusive events:

1) At time t there were $(Sn_{to} + k + 1)$ electrons in the traps and one electron was emitted to the conduction band during the interval $(t, t + \Delta t)$.
2) At time t there were $(Sn_{to} + k + 1)$ electrons in the traps and one electron was emitted to the valence band.
3) At time t there were $(Sn_{to} + k - 1)$ electrons in the traps and one electron was captured from the conduction band.
4) At time t there were $(Sn_{to} + k - 1)$ electrons in the traps and one electron was captured from the valence band.
5) At time t there were $(Sn_{to} + k)$ electrons in the traps and no transitions occurred.
6) During the interval $(t, t + \Delta t)$ two or more transitions occurred.

As usual the probability of the last event is assumed to be of smaller order of magnitude than Δt.

It is shown in Appendix B that to a linear approximation one additional electron in the traps produces an integrated change in the electron concentration at the surface of an amount

$$\int \delta n_s \, da = -\frac{n_{so}}{N_o + P_o} \qquad \text{(C.1a)}$$

and change in the hole concentration at the surface of

$$\int \delta p_s \, da = \frac{p_{so}}{N_o + P_o} , \qquad \text{(C.1b)}$$

where the integration is over the surface. This assumes quasi-equilibrium conditions, or times much longer than the lifetime, which is justified since we are concerned with the low frequency 1/f noise only. The rapid fluctuation in the carrier density due to generation-recombination processes is part of the shot noise. Therefore, when the number of electrons in the traps is $(Sn_{to} + k)$, we have approximately

$$\int_S n_s \, da \simeq Sn_{so} - k \frac{n_{so}}{N_o + P_o} \qquad \text{(C.2a)}$$

and

$$\int_S p_s \, da \simeq Sp_{so} + k \frac{p_{so}}{N_o + P_o} . \qquad \text{(C.2b)}$$

We will denote the probability that there are $(Sn_{to} + k)$ electrons in the traps at time t by $P_k(t)$ and make the usual assumption that the probability of future changes in the trap occupancy are independent of time and of past changes (i.e., assume a Markov process with stationary transition probabilities). Then the probability of event (1) occurring is given by the product of $P_{k+1}(t)$ and the probability that one electron was emitted to the conduction band during an interval of time Δt:

$$P_{k+1}(t)\left[Sn_{to} + k + 1\right] N_c c_n e^{-\frac{E_c - E_t}{kT}} \Delta t , \qquad \text{(C.3)}$$

where the notation is the same as that employed in Chapter II. Using the linear approximations (C.2), the probability of event (2) is

$$P_{k+1}(t)\left[Sp_{so} n_{to} + (k+1)\frac{p_{so} n_{to}}{N_o + P_o} + (k+1) p_{so}\right] c_p \Delta t . \qquad \text{(C.4)}$$

In a similar fashion we may compute all of the transition probabilities, finally obtaining for $P_k(t + \Delta t)$ the expression

$$P_k(t+\Delta t) = P_{k+1}(t)\left\{(S n_{to}+k+1)N_c c_n e^{-\frac{E_c-E_t}{kT}} + \left[S p_{so} n_{to} + (k+1)\frac{p_{so}n_{to}}{N_o+P_o} + (k+1)p_{so}\right]c_p\right\}\Delta t$$
$$+ P_{k-1}(t)\left\{\left[S n_{so} p_{to} - (k-1)\frac{n_{so}p_{to}}{N_o+P_o} - (k-1)n_{so}\right]c_n + (S p_{to}-k+1)N_v c_p e^{-\frac{E_t-E_v}{kT}}\right\}\Delta t \qquad \text{(C.5)}$$
$$+ P_k(t)\left\{1-\Delta t\left[(S n_{to}+k)\,c_n e^{-\frac{E_c-E_t}{kT}} + \left(S p_{so} n_{to} + k\frac{p_{so}n_{to}}{N_o+P_o} + k p_{so}\right)c_p\right.\right.$$
$$\left.\left. + \left(S n_{so} p_{to} - k\frac{n_{so}p_{to}}{N_o+P_o} - k n_{so}\right)c_n + (S p_{to}-k)N_v c_p e^{-\frac{E_t-E_v}{kT}}\right]\right\},$$

where terms of smaller order than Δt have been neglected. The terms due to the variation in $(E_c - E_t)$ have been neglected in accordance with (2.9).

So far we have written the equations in a general way which holds whether the trap density is large or small. However, using inequality (2.20), $n_{to}p_{to}/N_t \gg (N_o + P_o)$, and the inequalities which this one implies, namely $\delta n_t/n_{to} \ll 1$ and $\delta p_t/p_{to} \ll 1$, we can simplify (C.5) considerably:

$$P_k(t+\Delta t) = P_{k+1}(t)\left[S n_{to} N_c c_n e^{-\frac{E_c-E_t}{kT}} + S p_{so} n_{to} c_p + (k+1)\frac{p_{so}n_{to}c_p}{N_o+P_o}\right]\Delta t$$
$$+ P_{k-1}(t)\left[S n_{so} p_{to} c_n - (k-1)\frac{n_{so}p_{to}c_n}{N_o+P_o} + S p_{to} N_v c_p e^{-\frac{E_t-E_v}{kT}}\right]\Delta t \qquad \text{(C.6)}$$
$$+ P_k(t)\left\{1-\Delta t\left[S n_{to} N_c c_n e^{-\frac{E_c-E_t}{kT}} + S p_{so} n_{to} c_p + k\frac{p_{so}n_{to}c_p}{N_o+P_o}\right.\right.$$
$$\left.\left. + S n_{so} p_{to} c_n - k\frac{n_{so}p_{to}c_n}{N_o+P_o} + S p_{to} N_v c_p e^{-\frac{E_t-E_v}{kT}}\right]\right\}$$

Using the detailed balancing relations

$$n_{so} p_{to} c_n = n_{to} N_c c_n e^{-\frac{E_c - E_t}{kT}}$$

$$p_{so} n_{to} c_p = p_{to} N_v c_p e^{-\frac{E_t - E_v}{kT}} , \qquad (C.7)$$

and defining

$$\tau_n = \frac{N_o + P_o}{n_{so} p_{to} c_n} \qquad (C.8a)$$

$$\tau_p = \frac{N_o + P_o}{p_{so} n_{to} c_p} , \qquad (C.8b)$$

we obtain

$$\begin{aligned} P_k'(t) &= \lim_{\Delta t \to 0} \frac{P_k(t+\Delta t) - P_k(t)}{\Delta t} \\ &= P_{k+1}(t)\left[\frac{S(N_o+P_o)}{\tau} + \frac{k+1}{\tau_p}\right] - P_k(t)\left[\frac{2S(N_o+P_o)}{\tau} + \frac{k}{\tau_p} - \frac{k}{\tau_n}\right] \\ &\quad + P_{k-1}(t)\left[\frac{S(N_o+P_o)}{\tau} - \frac{k-1}{\tau_n}\right] , \end{aligned} \qquad (C.9)$$

where τ is the same quantity used in Chapter II and is given by (2.24).

The second step is to obtain a differential equation for the mean M(t) and the variance V(t) from the set (C.9). For M(t) this is done by multiplying (C.9) by k and summing over k. This gives

$$\begin{aligned} M'(t) &= \frac{S(N_o+P_o)}{\tau}(M-1) + \frac{1}{\tau_p}(V-M) - \frac{2S(N_o+P_o)}{\tau} M - \left(\frac{1}{\tau_p} - \frac{1}{\tau_n}\right) V \\ &\quad + \frac{S(N_o+P_o)}{\tau}(M+1) - \frac{1}{\tau_n}(V+M) \\ &= -\frac{M}{\tau} . \end{aligned} \qquad (C.10)$$

For the variance we multiply (C.9) by k^2 and sum. The terms in k^3 cancel, giving

$$V'(t) = \frac{2S(N_o+P_o)}{\tau} - \frac{2V}{\tau} + M\left(\frac{1}{\tau_p} - \frac{1}{\tau_n}\right) . \qquad (C.11)$$

The steady state value of V, denoted by V_o, is therefore $S(N_o + P_o)$.

If we denote by p_k the steady state probabilities (the solution of (C.9) with the left hand side zero) and by $P_{mk}(t)$ the probability that there are $(Sn_{to} + k)$ electrons in the traps at time t given that at time zero there were $(Sn_{to} + m)$ electrons in the traps, then the correlation function for the fluctuations in the trap occupancy is

$$R(t) = \sum_{m,k} mk\, p_m P_{mk}(t) \; . \tag{C.12}$$

Since $\sum_k k\, P_{mk}(t)$ is the mean at time t given that at time zero the mean was m, we have from (C.10)

$$\sum_k k P_{mk}(t) = m e^{-\frac{t}{\tau}} \; . \tag{C.13}$$

Hence

$$\begin{aligned} R(t) &= e^{-\frac{t}{\tau}} \sum m^2 p_m = e^{-\frac{t}{\tau}} V_o \\ &= S(N_o + P_o)\, e^{-\frac{t}{\tau}} \; . \end{aligned} \tag{C.14}$$

Taking the Fourier transform of (C.14) we get for the power spectrum (positive frequencies only)

$$G(\omega) = S(N_o + P_o) \frac{4\tau}{1 + (\omega\tau)^2} \; . \tag{C.15}$$

REFERENCES

1. A. van der Ziel, Noise (Prentice Hall, Inc., New York, 1954), p. 204.
2. B. V. Rollin and I. M. Templeton, Proc. Phys. Soc. B66, 259 (1953).
3. T. E. Firle and H. Winston, Bull. Am. Phys. Soc. 30, No. 2, 44 (1955).
4. Van Vliet, Van Leeuwen, Blok and Ris, Physica 20, 481 (1954).
5. P. H. Miller, Proc. I.R.E. 35, 252 (1947).
6. I. M. Templeton and D. K. C. MacDonald, Proc. Phys. Soc. B66, 680 (1953).
7. B. R. Russell, Tenth Ann. Conf. on Phys. Electronics, M.I.T., March 30 - April 1, 1950.
8. H. C. Torrey and C. A. Whitmer, Crystal Rectifiers, M.I.T. Rad. Lab. Series (McGraw-Hill Book Co., New York, 1948), Vol. 15, Ch. 6.
9. H. C. Montgomery, Bell Syst. Tech. J. 31, 950 (1952).
10. H. A. Gebbie, Bull. Am. Phys. Soc. 30, No. 2, 44 (1955).
11. J. Bernamont, Proc. Phys. Soc. 49 (extra part), 138 (1937).
12. A. van der Ziel, Physica 16, 359 (1950).
13. F. K. duPré, Phys. Rev. 78, 615 (1950).
14. F. Seitz, The Modern Theory of Solids (McGraw-Hill Book Co., New York, 1940), p. 495.
15. J. M. Richardson, Bell Syst. Tech. J. 29, 117 (1950).
16. L. Bess, Phys. Rev. 91, 1569 (1953).
17. G. G. Macfarlane, Proc. Phys. Soc. B63, 807 (1950).
18. R. E. Burgess, Proc. Phys. Soc. B66, 334 (1953).
19. W. Shockley, Electrons and Holes in Semiconductors (D. Van Nostrand Co., New York, 1950), p. 342.
20. H. Suhl, Bell Syst. Tech. J. 32, 647 (1953).
21. G. B. Herzog and A. van der Ziel, Phys. Rev. 84, 1249 (1951). See also R. H. Mattson and A. van der Ziel, J. Appl. Phys. 24, 222 (1953).
22. H. C. Montgomery, private communication.

23. T. G. Maple, L. Bess, and H. A. Gebbie, J. Appl. Phys. 26, 490 (1955).

24. D. P. Kennedy, A.I.E.E. Winter Meeting, New York, Jan. 18-22, 1954.

25. J. Bardeen, Phys. Rev. 71, 717 (1947).

26. W. Shockley and G. L. Pearson, Phys. Rev. 74, 232 (1948).

27. W. H. Brattain and J. Bardeen, Bell Syst. Tech. J. 32, 1 (1953).

28. S. R. Morrison, R. Sun, and J. Bardeen, Tech. Report No. 5, Contract N6-ori-07140, E.E. Res. Lab., Univ. of Illinois (15 January 1955).

29. G. G. E. Low, Proc. Phys. Soc. B68, 10 (1955).

30. R. H. Kingston and A. L. McWhorter, Bull. Am. Phys. Soc. 30, No. 1, 52 (1955).

31. W. L. Brown, Bull. Am. Phys. Soc. 30, No. 2, 42 (1955).

32. H. C. Montgomery and W. L. Brown, Bull. Am. Phys. Soc. 30, No. 2, 42 (1955).

33. R. H. Kingston, Phys. Rev. 94, 1416 (1954).

34. R. H. Kingston, to be published in Phys. Rev., May 15, 1955.

35. G. A. deMars, H. Statz, and L. Davis, Phys. Rev. 98, 539 (1955).

36. H. Statz, L. Davis, and G. A. deMars, Phys. Rev. 98, 540 (1955).

37. M. Green, private communication.

38. H. Y. Fan, Phys. Rev. 92, 1424 (1953).

39. J. A. Hornbeck and J. R. Haynes, Phys. Rev. 97, 311 (1955).

40. P. H. Miller, Semi-Annual Report No. 8 on Semicond. Res., Dept. of Physics, Univ. of Penn. (December, 1954).

41. W. Shockley and W. T. Read, Phys. Rev. 87, 835 (1952).

42. W. Shockley, Bell Syst. Tech. J. 28, 435 (1949).

43. J. R. Schrieffer, Phys. Rev. 97, 641 (1955).

44. T. G. Maple, Quarterly Progress Report on Solid State Research, Lincoln Laboratory, M.I.T., 1 November 1954, p. 12.

45. A. L. McWhorter and R. H. Kingston, Proc. I.R.E. 42, 1376 (1954).

46. J. T. Law, Proc. I.R.E. 42, 1367 (1954).

47. W. L. Brown, Phys. Rev. 91, 518 (1953).

48. H. Christensen, Proc. I.R.E. 42, 1371 (1953).

49. International Critical Tables (McGraw-Hill Book Co., New York, 1926), Vol. 1, p. 67.

50. H. Statz, private communication.

51. R. Holm, J. Appl. Phys. 22, 569 (1951).

52. N. F. Mott, Trans. Far. Soc. 43, 429 (1947).

53. N. Cabrera, Phil. Mag. 40, 175 (1949).

54. S. Machlup, J. Appl. Phys. 25, 341 (1954).

55. W. Feller, An Introduction to Probability Theory and its Applications (John Wiley and Sons, Inc., New York, 1950), Ch. 17.

BIOGRAPHICAL NOTE

Alan L. McWhorter was born in Crowley, Louisiana, on August 25, 1930. He received the B.S. degree in electrical engineering from the University of Illinois in 1951, and the following year began studying for an Sc.D. degree in electrical engineering at the Massachusetts Institute of Technology. During the summer of 1953 he worked at the Philips Research Laboratory in Eindhoven, Holland, on an M.I.T. Overseas Summer Fellowship. Since then he has been a Research Assistant in the Research Laboratory of Electronics and has also been closely associated with Lincoln Laboratory. Previously he had worked at Lincoln Laboratory on the microwave applications of ferrites.

Mr. McWhorter is a member of the American Physical Society, Tau Beta Pi, and Eta Kappa Nu.